Novel 5-HT$_7$ Receptor Inverse Agonists. Synthesis and Molecular Modeling of Arylpiperazine- and 1,2,3,4-Tetrahydroisoquinoline-Based Arylsulfonamides

Erik S. Vermeulen,*,§ Marjan van Smeden,§ Anne W. Schmidt,‡ Jeffrey S. Sprouse,‡ Håkan V. Wikström,§ and Cor J. Grol§

Department of Medicinal Chemistry, Center for Pharmacy, State University of Groningen, A. Deusinglaan 1, NL-9713 AV Groningen, The Netherlands, and Pfizer Global R & D, Department of Neuroscience, MS 8220-4178, Groton, Connecticut 06340

Received April 2, 2004

A series of arylpiperazine- and 1,2,3,4-tetrahydroisoquinoline-based arylsulfonamides was synthesized and evaluated for their interactions with the constitutively active 5-HT$_7$ receptor. Effects on basal adenylate cyclase activity were measured using HEK-293 cells expressing the rat 5-HT$_7$. All ligands produced a decrease of adenylate cyclase activity, indicative of their inverse agonism. Additionally, computational studies with a set of 22 inverse agonists, including these novel inverse agonists and inverse agonists known from literature, resulted in a pharmacophore model and a CoMFA model ($R^2 = 0.97$, SE = 0.18). Docking of inverse agonists at the binding site of a model of the helical parts of the 5-HT$_7$ receptor, based on the α carbon template for 7-TM GPCRs, revealed interesting molecular interactions and a possible explanation for observed structure−activity relationships.

Introduction

In the process of characterization of the 5-HT$_7$ receptor, discovered over a decade ago,[7,29,35,36,39] our attention was drawn to the development ligands based on the structure of 1,2,3,4-tetrahydroisoquinoline (THIQ) and 2-methoxyphenylpiperazine (2-MPP) linked with a spacer to a number of divergent arylsulfonamides. The onset to this approach was encouraged by the results obtained from studies on the closely related 5-HT$_{1A}$ receptor.[8,9,30−33] These studies revealed that replacement of the arylpiperazine moieties of known serotonergic drugs by the THIQ nucleus resulted in potent inhibitors of subtypes of the extensive family of 5-HT receptors. Simultaneously, the outcome of research projects in the area of 5-HT$_7$ receptor antagonism suggested that aromatic (sulfon-)amides with different alkyl chains as spacer between this moiety and a positively charged nitrogen-containing group proved to be potent ligands for this receptor subtype.[12,26,48] This supported the idea that ligands could be developed based on both arylpiperazines and THIQs that would affect adenylate cyclase activity mediated by the 5-HT$_7$ receptor. Although its (patho-)physiological role still remains unclear, it has been demonstrated that the 5-HT$_7$ receptor is constitutively active, and that basal adenylate cyclase activity was reduced by increased concentrations of 5-HT antagonists (inverse agonists) in membranes of stable cell lines expressing the human 5-HT$_7$ receptors.[22,21,44] Moreover, a number of recently developed ligands showed a small apparent reduction in basal adenylate cyclase activity in the absence of agonists during pharmacological profiling as well,[19,20,28,44] indicating these compounds should be referred to as inverse agonists instead of (neutral) antagonists. Several of these inverse agonists have been used recently to derive pharmacophore models for 5-HT$_7$ receptor antagonism.[26,27]

We wish to report the development and pharmacological characterization of novel 5-HT$_7$ receptor inverse agonist based on the structure of THIQ and 2-MPP and present a pharmacophore model on the basis of inverse agonists only. Additional computational studies (CoMFA, receptor modeling, docking of inverse agonist at the binding site) suggested plausible explanations for observed structure−activity relationships (SAR) and showed interesting similarities with our recently published pharmacophore model for 5-HT$_7$ receptor agonism.[47]

Ligands. The geometry of the first pharmacophoric hypothesis for 5-HT$_7$ receptor antagonism[26] was the reference point for the development of two series of ligands, based on 2-MPPs and THIQs. Additionally, a small set of miscellaneous inverse agonists was collected from previous in-house studies that were actually designed as potential agonists, but unexpectedly decreased 5-HT$_7$ receptor-mediated basal adenylate cyclase activity.

The chemical structure of 2-MPPs is well-known for its affinity to several members of the family of serotonergic receptors. Recently, it was demonstrated that ligands possessing this structure interact with the 5-HT$_7$ receptor as well.[17,26,34] SAR studies with these ligands revealed an optimal spacer length of four or five carbon atoms to link the 2-MPPs with aryl-substituted ketones, tetrahydrobenzindoles or naphtholactams and naphthosultams. However, aiming at ligands in which the 2-MPP moiety is linked to an aryl sulfonamide, it was hypothesized that the spacer between the positively ionizable nitrogen atom of the piperazine ring and the sulfonamide moiety should consist of three carbon atoms, matching the recently published selective 5-HT$_7$ receptor ligands.[12,13,15,28,45,46] Therefore 2-MPP-based ligands **12** and **13a**−**c** (Chart 1) were developed with

* To whom correspondence should be addressed. Tel: +31 50 311 8007, fax: +31 50 360 0390, e-mail: e.s.vermeulen@farm.rug.nl.
§ State University of Groningen.
‡ Pfizer Global R & D.

10.1021/jm049743b CCC: $27.50
Published on Web 09/23/2004

Chart 1. Chemical Structure of the 5-HT_7 Receptor Ligands **1a**−**c**, **2**, **3a,b**, **9**, **10a**−**c**, **14a**−**h**, **19**, **20**, **25**, and **32**

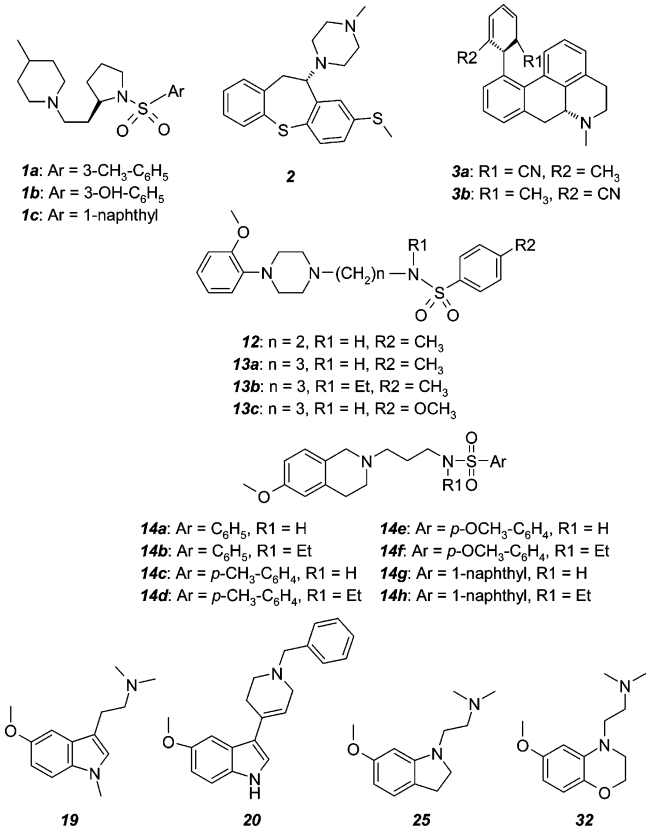

differently substituted arylsulfonamides and a C_3 (and C_2) alkyl chain connecting both moieties.

Analogously, a series of 5-HT_7 receptor ligands was developed containing the THIQ structure with a methoxy substituent at the 6-position (**14a**−**h**, Chart 1). As mentioned earlier, the structure had shown to be a good replacement for the arylpiperazine moiety in 5-HT_{1A} receptor ligands,[8,9,30−33] and produce potent 5-HT_7 receptor ligands when linked to tetrahydrobenzindoles as well.[18] Variation of the arylsulfonamide moiety coupled to the THIQ nucleus by a C_3 spacer would offer additional information on the SAR of these ligands. In addition, substitution of the sulfonamide nitrogen in both series of novel 5-HT_7 receptor ligands by a simple ethyl substituent was investigated to mimic the steric and lipophilic effect of the chiral pyrrolidine ring present in the previously developed sulfonamides without the necessity to separate enantiomers.

A small number of diverse ligands (**19**, **20**, **25**, **32**, Chart 1) from previous studies, which were tested for their ability to affect 5-HT_7 receptor-mediated adenylate cyclase activity, appeared to decrease basal activity levels as well. Finally, the highly rigid and potent 5-HT_7 receptor inverse agonist (*S*)-methiothepin (**2**) and the aporphine derivative **3b** (Chart 1)[25] served as templates to select the active conformation of the far more flexible ligands with long alkyl chains. Though at first sight structurally not closely related, the results of the fitting procedure indicate several striking similarities among the chemical structures of the set of ligands used to build the pharmacophore model.

Chemistry. The synthetic procedures leading to the target compounds **12**, **13a**−**c** and **14a**−**h** are illustrated in Scheme 1. Synthesis of both series of sulfonamides started off with either a simple nucleophilic substitution of the secondary amines of 2-MPP or 6-methoxy-THIQ (prepared by Pictet−Spengler cyclization of the 3-methoxyphenethylamine with formaldehyde) with bromoacetonitrile or with a Michael addition with acrylonitrile. While the methylene nitrile ***6*** was easily reduced to the primary amine using only $LiAlH_4$ in ether or THF, application of the same conditions on the nitriles **7** and **8** obtained from Michael addition resulted in serious

Scheme 1. Synthesis of Target Compounds **12**, **13a**−**c** and **14a**−**h**[a]

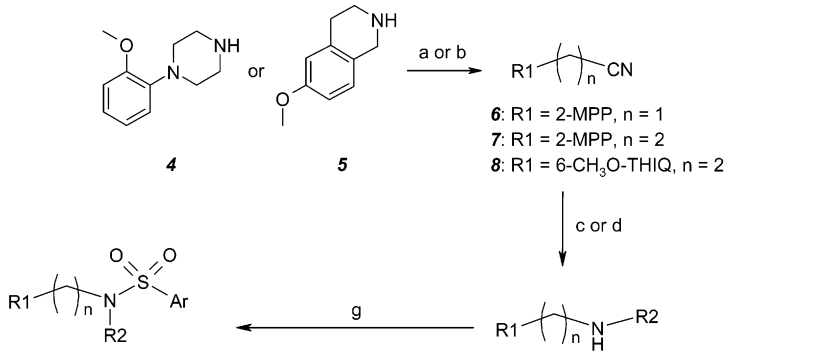

[a] Reagents and conditions: (a) Bromoacetonitrile, K_2CO_3, KI, acetonitrile, reflux. (b) Acrylonitrile, ethanol, reflux. (c) $LiAlH_4$, ether or THF, rt. (d) $LiAlH_4$, $AlCl_3$, ether, rt. (e) Ac_2O, $NaHCO_3$, (saturated aqueous solution), CH_2Cl_2. (f) $LiAlH_4$, THF, reflux. (g) $ArSO_2Cl$, $NaHCO_3$, (saturated aqueous solution), CH_2Cl_2.

Scheme 2. Synthesis of Target Compounds **19** and **20**[a]

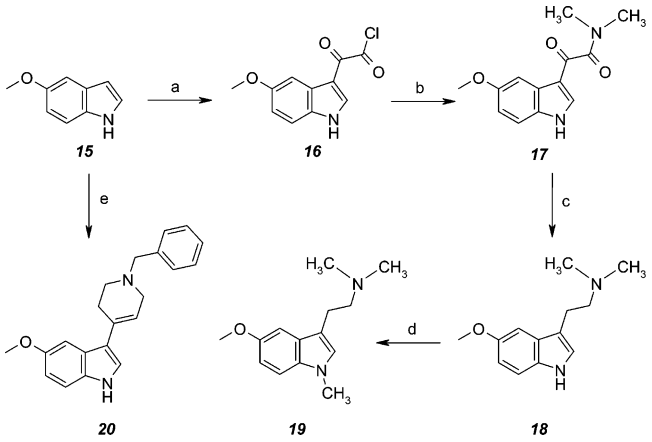

[a] Reagents and conditions: (a) Oxalyl chloride, diethyl ether. (b) Dimethylamine hydrochloride, $NaHCO_3$ (sat.)/$CHCl_3$. (c) $LiAlH_4$, THF. (d) KO-t-Bu, dimethyl oxalate, DMF, reflux. (e) *N*-Benzylpiperidone, $NaOCH_3$, CH_3OH, reflux.

amounts of cleavage, yielding primarily starting materials. Therefore, the conditions were modified using 1 equiv of $AlCl_3$ in combination with $LiAlH_4$. Coupling of the primary amine with the appropriate arylsulfonyl chloride was straightforward. In case substitution of the sulfonamide nitrogen was desired, acetylation and subsequent reduction of the acetamide prior to coupling with the arylsulfonyl chloride was preferred, due to serious decrease of nucleophilicity of the sulfonamide nitrogen. Coupling of the primary and secondary amines with sulfonyl chlorides in an alkaline two-phase system proceeded with complete conversion to the sulfonamide end products. Overall yields of these reactions were in the range of 60−75%.

The syntheses of indole-based target compounds **19** and **20** started with 5-methoxyindole (Scheme 2). A classical tryptamine synthesis pathway[41] was followed, using oxalyl chloride and dimethylamine. Subsequent reduction of the intermediate **17** yielded the 5-HT$_7$ receptor agonist **18**.[47] Methylation of the indole-NH with dimethyl sulfate under alkaline conditions gave the target compound **19**. Notably, when methylation of 5-methoxyindole was performed, followed by functionalization with oxalyl chloride and dimethylamine, reduction of the intermediate 2-oxo-acetamide did not go to completion, but stopped at the level of 2-hydroxyethylamine, even at elevated temperatures and with a large excess of $LiAlH_4$.

Ligand **20** was prepared in a single step using *N*-benzylpiperidone in the presence of sodium methoxide.

Indoline **25** was prepared from 6-methoxyindole, which was reduced with $NaCNBH_3$ in glacial acetic acid to the indoline (Scheme 3). Subsequent substitution of the nitrogen atom with an ethylamine side chain proceeded via the 2-chloroacetylated intermediate. Like the reduction of nitriles **7** and **8**, reduction of the amide group at this stage required mild conditions using AlH_3 (prepared from $LiAlH_4$ and $AlCl_3$) to prevent cleavage of the amide bond.

Finally, the benzoxazine-based ligand **32** was synthesized from the commercially available 2-nitro-4-methoxyphenol in a straightforward process: catalytic hydrogenation of the nitro group to the 2-amino-4-

Scheme 3. Synthesis of Target Compound **25**[a]

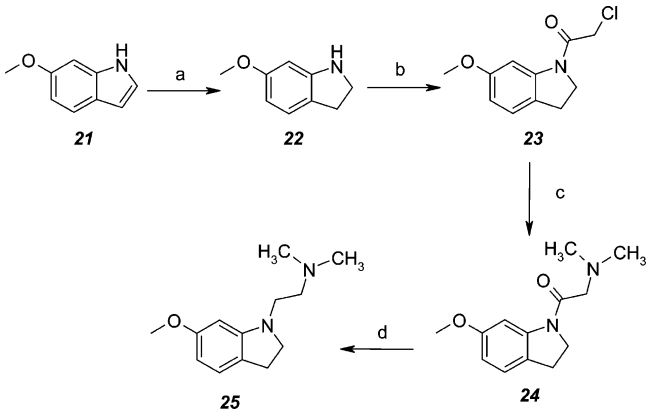

[a] Reagents and conditions: (a) $NaCNBH_3$, AcOH. (b) Chloroacetyl chloride, K_2CO_3, CH_2Cl_2. (c) dimethylamine hydrochloride, K_2CO_3, AcCN. (d) $LiAlH_4$, $AlCl_3$, THF.

methoxyphenol was followed by ring closure under alkaline conditions with 2-chloroacetyl chloride (Scheme 4). Subsequent reduction of **28** yielded the key intermediate **29**. Functionalization occurred via the same pathway as applied for target compound **25**. Again, reduction in the final step turned out to be delicate, but using the same modifications as before, the target compounds could be obtained successfully.

3-D QSAR of 5-HT$_7$ Receptor Inverse Agonists. Using the set of ligands depicted in Chart 1, CoMFA studies were performed to investigate three-dimensional qualitative structure−activity relationships (3-D QSAR). Therefore, the same methods were applied as recently described.[47] Full conformational analysis of the set of 5-HT$_7$ receptor inverse agonists in their protonated form was performed in MacroModel,[2] and followed by a pharmacophore identifying procedure through ligand overlap using APOLLO.[40] Since the nature of the set of newly synthesized ligands is rather flexible due to the presence of C_2 and C_3 spacers, the search for the active conformation of ligands **1a**−**c**, **12**, **13a**−**c**, **14a**−**h**, **19**, **20**, **25**, and **32** was guided by fitting these ligands with the rigid structures of **2** and **3a**,**b**, and verified by the recently published dimensions of the optimized pharmacophore model for 5-HT$_7$ receptor antagonism.

Both oxygen atoms of the sulfonamide containing ligands were defined as H-bond-accepting moieties (HBA). In case of absence of this moiety in **19**, **20**, **25**, and **32**, the oxygen of the methoxy group at the six-membered aromatic ring served this purpose. The protonated, positively charged nitrogen atom present in all ligands was defined as H-bond-donating (PI) moiety. Centroids were defined for the aromatic ring next to the sulfonamide moiety and the chiral five-membered heterocyclic rings (**1a**−**c**), while those ligands lacking this moiety were equipped with a centroid through the six-membered aromatic ring(s) of the indol(-in-)e (**19**, **20**, and **25**), the benzoxazine (**32**), the aporphines (**3a**,**b**), and the (*S*)-methiothepin (**2**) core structure. In these cases, the best fit of these centroids with the centroid defined for the five-membered chiral pyrrolidine ring of **1a**−**c** was calculated. The superpositioned ligands after the fitting procedure, and surrounded by their mutual interaction points by means of water molecules, are depicted in Figure 1. The set of superimposed

Scheme 4. Synthesis of Target Compound **32**[a]

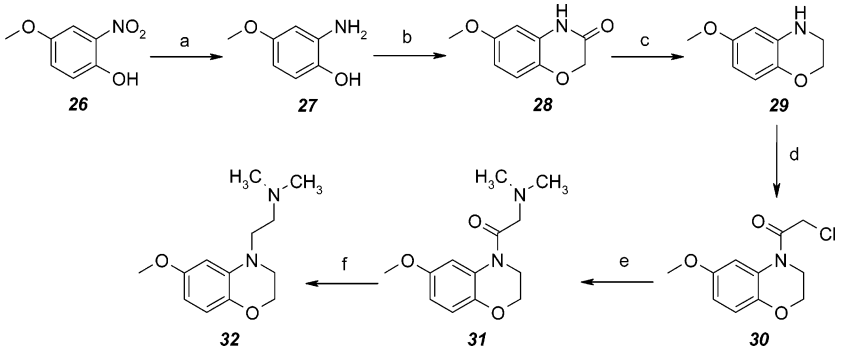

[a] Reagents and conditions: (a) Pd/C, H_2, EtOH. (b) 2-Chloroacetyl Chloride, K_2CO_3, AcCN, reflux. (c) $LiAlH_4$, THF, rt. (d) 2-Chloroacetyl chloride, pyridine (e) Amine, K_2CO_3, AcCN, rt. (f) $LiAlH_4$, $AlCl_3$, THF, rt.

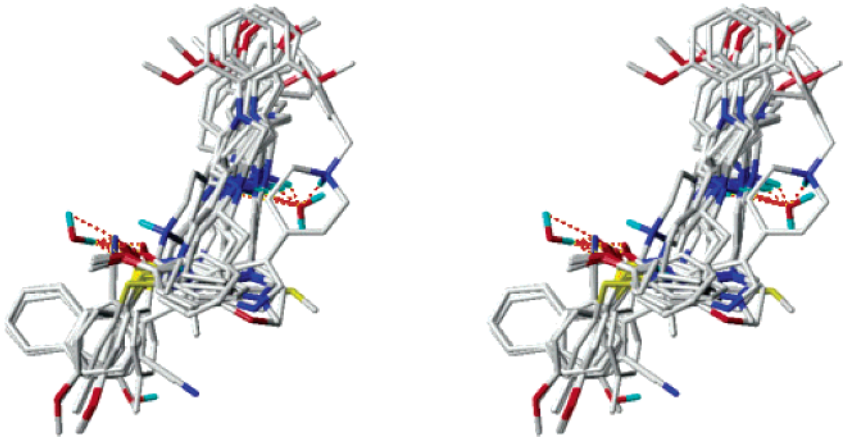

Figure 1. Stereo picture of the best fit of ligands **1a**−**c**, **2**, **3a**,**b**, **12**, **13a**−**c**, **14a**−**h**, **19**, **20**, **25** and **32**. H-bonds with mutual interaction points depicted in dotted lines. Nonessential hydrogen atoms have been omitted.

ligands was subsequently used for CoMFA computations using the Sybyl molecular modeling software program[3].

Receptor Modeling: Docking of 5-HT$_7$ Receptor Inverse Agonists at Binding Site. The recently published model of the helical parts of the 5-HT$_7$ receptor,[47] based on the template of α-carbon atoms of the TM domains of GPCRs,[5] was used to study the molecular interactions of the inverse agonists at the binding site of the model (see ref 47 for motivation). Manual docking of the inverse agonist into the binding site was guided by the 3-D orientation of the mutual interaction points surrounding the set of ligands from the APOLLO fitting procedure. The putative binding site residue interacting with the HBA moieties of the inverse agonists was oriented at the position of threonine 244 (Thr$^{5.43}$, numbering according to highly conserved amino acid residues throughout family of GPCRs[6]) of TM5, while the mutual interaction point of the positively charged nitrogen atom (PI) was superpositioned at aspartate 162 in TM3 (Asp$^{3.32}$). Subsequent minimization of the receptor−ligand complex resulted in properly docked ligands and revealed several interesting ligand binding interactions additional to the supposed interactions with Asp$^{3.32}$ and Thr$^{5.43}$.

Receptor Modeling: CoMFA Mapping onto the 5-HT$_7$ Receptor Binding Site. The CoMFA model was projected onto the binding site to identify conceivable amino acid residues that could account for the contour maps as computed during the comparative molecular field analysis. For this purpose as well, the three-dimensional orientation of mutual interaction points, as calculated from the preceding alignment procedure by APOLLO, were used to locate the ligand binding amino acid residues in the receptor binding site. Careful examination of this projection onto the inner sphere of the binding site basically indicated the most distinguishing amino acid residues.

Pharmacology. All target compounds were evaluated at Pfizer laboratories for their ability to compete for [^{3}H]5-CT binding to cloned rat 5-HT$_7$ receptors expressed in HEK-293 cells. Additionally, the effect on adenylate cyclase activity relative to the effects of (*S*)-methiothepin (**2**) was determined. Basal levels of cAMP production equaled 24 pmol min^{-1} mg^{-1} protein. This was reduced by **2** to 5 pmol min^{-1} mg^{-1} protein at a ligand concentration of 1.0×10^{-5} M. This reduction served as reference reduction level (100%) for all other target compounds.

Results and Discussion

Despite the heterogeneity of the chemical structures of the 22 ligands used for the pharmacophore identification for 5-HT$_7$ receptor inverse agonism by APOLLO, the calculations resulted in an ensemble of well-fitted ligands surrounded by their mutual interaction points mimicking the putative amino acid residues of the binding site (Figure 1). Quite notable is the irregular orientation of **20** with its benzyl-substituted tetrahydropyridine ring out of line with the remainder of the ligands. Additionally, the neighboring aromatic rings of **2** and **3a**,**b** appear to match well with the aromatic ring of the sulfonamide containing ligands on one hand and

the chiral, five-membered heterocyclic ring of **1a**−**c** on the other hand. The variety in orientation of the arylpiperazine and THIQ moieties and other 3D-QSAR is reflected by the results of the CoMFA computations discussed later in this section.

Data listed in Table 1 clearly indicate that both the 1,2,3,4-tetrahydroisoquinoline and the arylpiperazine target compounds can make good 5-HT$_7$ receptor ligands with potent inverse agonist characteristics. Generally, the average values of the distances between the pharmacophoric features of the ligands **1a**−**c**, **2**, **3a**,**b**, **12**, **13a**−**c**, **14a**−**h**, **19**, **20**, **25**, and **32** are close to the corresponding values of recently published models.[26,27] The data also indicate that the sulfonamides **12** and **13a**−**c** act as potent inverse agonists with a C_2 or a C_3 alkyl chain bridging the arylpiperazine moiety and the arylsulfonamide moiety. This latter geometry matches well with the corresponding distance between HYD*4* and PI of the initial pharmacophore model,[26] but contrasts with the optimum value of four to five carbon atoms reported earlier.[17,26,34]

Another important SAR that can be deducted from the current series of ligands is the presence of the hydrophobic substituent at the nitrogen of the sulfonamide (HYD1). Ligands lacking this feature (**12**, **13a**, **14c**, **14e**, and **14g**) show considerable lower affinities than their ethyl-substituted analogues. As for the different aryl groups of the arylsulfonamides, no large differences in binding affinities can be detected, except for **1b**, which has a hydrogen bond (H-bond)-donating group at the meta-position relative to the sulfonamide moiety.

In the case of the aporphine ligands **3a**,**b**, it was hypothesized that the nitrogen atom of the nitrile substituent could serve as H-bond-accepting moiety. However, the different orientation of this substituent and the correlated increased distance between this moiety (HBA) and the positively charged nitrogen and its substituent (PI and HYD2, respectively) in the case of the more potent atropisomers **3b** indicate this interaction is of no concern in this case, or the positive effect of H-bond formation of **3a** is canceled out by the methyl substituent when oriented in the opposite direction.

The computational studies performed with the set of ligands listed in Table 1 resulted in a CoMFA model with a good correlation between actual and predicted pK_i values (Figure 3, $R^2 = 0.97$, standard error of estimate = 0.18 (not cross-validated)). The optimum number of components equaled 6, and 52 out of 2808 columns were dropped during PLS analysis. The ratio of steric and electrostatic effects equaled 0.60:0.40. Stereo pictures of ligand **1b** and **14e** (Figure 2, upper and lower panel respectively) are illustrative.Both ligands have the oxygen atoms closely oriented toward the areas indicative of the favorable effect of electronegative charge. Furthermore, the five-membered pyrrolidine ring of **1b** perfectly occupies the area indicating the favorable effect of the hydrophobic group (HYD1), which is absent in case of **14e**. An additional characteristic of the low affinity ligand **14e** is the orientation of the substituted THIQ moiety far into the areas that identify the negative influence of bulky groups in that area. Obviously, these areas indicate the boundaries of the lipophilic pocket hosting HYD2 and HYD3 of the pharmacophore model that are respected by **1b**, but surpassed by **14e**. With respect to these latter CoMFA areas, it should be noted that the orientation of the THIQ and arylpiperazine moieties is differing slightly throughout the series and is influenced by the absence or presence of an aliphatic substituent at the sulfonamide nitrogen atom. Those ligands that do not have their hydrophobic substituent oriented precisely within the boundaries of these areas (**14c**, **14e**, and **14g**) significantly show lower affinity for the 5-HT$_7$ receptor. The lower value of the predictive power of this model (Table 2, $q^2 = 0.64$, standard error of estimate = 0.60 (cross-validated, set of ligands randomly divided into two groups)) is most probably the result of the dissimilarities of ligands **19**, **20**, **25**, and **32** compared to the large number of arylsulfonamide ligands.

The mapping of the CoMFA areas onto the model of the TM domains of the 5-HT$_7$ receptor offers a practical method of correlating both models (Figure 4). The yellow areas surrounding the 2-MPP and THIQ moieties indicate the boundaries of the lipophilic pocket hosting HYD2 and HYD3 of the pharmacophore model and can be superpositioned perfectly onto side chains of amino acid residues Ile159 (Ile$^{3.29}$) of TM3 and Phe369 (Phe$^{7.38}$) and Leu370 (Leu$^{7.39}$) of TM7. Additionally, the red area indicating the favorable effect of electronegative charge in the vicinity of the oxygen atoms of the sulfonamide moiety are projected nicely onto the side chain of the H-bond-donating residue Thr244 of TM5 (Thr$^{5.43}$), while the green area indicating the favorable effect of bulk, representing HYD1, is close to TM6 and surrounded by Phe336 (Phe$^{6.44}$) at the bottom and Trp340 (Trp$^{6.48}$) at the top of this lipophilic pocket.

In close-up, after minimization of the receptor−ligand complex, the molecular interactions of **1b** and the binding site of the 5-HT$_7$ receptor are depicted in Figure 5. The electrostatic interactions between the protonated nitrogen atom and the negatively charged Asp162 (Asp$^{3.32}$), the sulfonamide oxygen and the hydroxyl group of Thr244 (Thr$^{5.43}$), and in particular the hydroxyl group at the meta position of the six-membered aromatic ring of **1b** and the side chain of Thr337 (Thr$^{6.45}$) are depicted in dotted lines. This latter H-bonding feature was identified earlier by SAR studies in which the hydroxyl-substituted **1b** showed a substantial increase in 5-HT$_7$ receptor affinity compared to its methoxy-substituted analogue.[28] From the current molecular modeling studies it could be suggested that the latter methoxy-substituted analogue could accept a H-bond donated by Thr$^{6.45}$ as well, but the favorable effect of this H-bond is most probably abolished by steric repulsions between the methyl group and TM6. Interestingly, in case of the aporphine ligand **3b**, it was observed after minimization of the receptor−ligand complex that a H-bond was formed as well between the nitrogen atom of the nitrile substituent and Thr337 (Thr$^{6.45}$) instead of Thr$^{5.43}$ (which forms a H-bond with the HBA groups of all other ligands). This might explain the higher binding affinity compared to its atropisomer **3a**. The conformation of **3a** would be capable of forming a H-bond with Thr$^{5.43}$, but steric repulsion of the methyl substituent with the relatively narrower inter helical space between TM5 and TM6 eventually results in a lower affinity for the 5-HT$_7$ receptor than **3b**.

Table 1. Calculated Physical Properties, Geometries, Experimental 5-HT$_7$ Receptor Binding Affinities and Relative Potencies of Basal Adenylate Cyclase Stimulation of Compounds **1a**−**c**, **2**, **3a**,**b**, **12**, **13a**−**c**, **14a**−**h**, **19**, **20**, **25**, and **32**

compd	Ar	spacer	R1	HYD1−HYD2	HYD1−HYD3	HYD1−HYD4	HYD1−HBA	HYD1−PI	HYD2−HYD3	HYD2−HYD4	HYD2−HBA	HYD2−PI	HYD3−HYD4	HYD3−HBA	HYD3−PI	HYD4−HBA	HYD4−PI	HBA−PI	log *P* (calc)	pK_a (calcd)	K_i (nM)	cAMP (%)[a]
1a	3-CH_3-C_6H_4			6.14[n]	8.91[f]	4.61	3.50	4.83	2.90[f]	9.30	6.02	1.45	12.18[f]	8.78[f]	4.28[f]	3.82	8.05	5.04	3.7	10.4	3[n]	n.d.[n]
1b	3-OH-C_6H_4			6.14[d]	8.91[f]	4.61	3.50	4.83	2.90[f]	9.30	6.02	1.45	12.18[f]	8.78[f]	4.28[f]	3.82	8.05	5.04	2.7	10.4	1[n]	n.d.[n]
1c	1-naphthyl			6.17	9.00	4.76	3.46	4.86	2.90[f]	9.28	5.73	1.45	12.13[f]	8.46[f]	4.35[f]	3.80	8.10	4.76	4.2	10.4	10[n]	n.d.[n]
2				7.43	n.d.	4.73	3.16	5.96	n.d.	9.67	8.62	1.49	n.d.	n.d.	n.d.	3.17	8.28	7.22	3.4	8.1	1	-100[d]
3a				5.53	n.d.	4.29	4.06	5.10	n.d.	8.66	6.06	1.50	n.d.	n.d.	n.d.	3.88	7.66	5.45	6.1	7.3	21[n]	n.d.
3b				5.67	n.d.	4.29	4.17	5.11	n.d.	8.71	9.38	1.50	n.d.	n.d.	n.d.	3.88	7.69	8.45	6.1	7.3	4[n]	n.d.
12	4-CH_3-C_6H_4	C_2	H	n.d.	n.d.	n.d.	n.d.	n.d.	4.09	8.97	6.19	1.41	12.95	10.10	5.51	3.83	7.64	4.95	2.2	7.4	75	-66[c]
13a	4-CH_3-C_6H_4	C_3	H	n.d.	n.d.	n.d.	n.d.	n.d.	4.06	9.36	6.23	1.41	13.03	9.49	5.47	3.82	8.10	5.26	2.6	7.5	52	-20[c]
13b	4-CH_3-C_6H_4	C_3	Et	7.03	10.96	3.85	3.65	5.76	4.09	9.21	5.61	1.42	12.78	8.97	5.51	3.83	8.13	5.12	3.3	7.7	19	-93[d]
13c	4-OCH_3-C_6H_4	C_3	H	n.d.	n.d.	n.d.	n.d.	n.d.	4.09	10.02	7.25	1.42	13.77	10.96	5.51	3.78	8.79	6.11	2.1	7.5	100	-35[d]
14a	C_6H_5	C_3	H	n.d.	n.d.	n.d.	n.d.	n.d.	2.49	9.40	6.28	1.43	11.58	8.35	3.79	3.82	8.10	5.26	2.3	7.0	75	-36[c]
14b	C_6H_5	C_3	Et	7.13	9.55	4.08	3.12	5.97	2.48	9.37	6.42	1.44	11.53	8.47	3.79	3.81	8.05	5.38	3.1	7.4	54	-93[c]
14c	4-CH_3-C_6H_4	C_3	H	n.d.	n.d.	n.d.	n.d.	n.d.	2.48	9.40	6.29	1.44	11.58	8.35	3.79	3.82	8.10	5.27	3.0	7.0	520	-61[b]
14d	4-CH_3-C_6H_4	C_3	Et	7.13	9.55	4.08	3.13	5.97	2.48	9.37	6.42	1.44	11.53	8.47	3.79	3.81	8.05	5.38	3.8	7.4	11	-95[d]
14e	4-OCH_3-C_6H_4	C_3	H	n.d.	n.d.	n.d.	n.d.	n.d.	2.48	10.02	7.21	1.44	11.52	8.81	3.79	3.78	8.79	6.06	2.5	7.0	1200	-84[b]
14f	4-OCH_3-C_6H_4	C_3	Et	7.06	9.32	3.86	3.65	5.75	2.48	9.22	5.61	1.44	10.96	7.24	3.79	3.84	8.13	5.76	3.3	7.4	29	-94[d]
14g	1-naphthyl	C_3	H	n.d.	n.d.	n.d.	n.d.	n.d.	2.48	9.38	5.95	1.44	11.19	7.64	3.79	3.80	8.23	5.05	3.6	7.0	360	-104[b]
14h	1-naphthyl	C_3	Et	6.32	8.61	4.87	3.03	5.09[k]	2.48	9.21	5.94	1.44	10.83	7.64	3.79	3.83	8.12	5.06	4.3	7.4	19	-91[d]
19				6.47[k,m]	n.d.	n.d.	2.77[k]	6.02[k]	n.d.	n.d.	7.04[m]	0.86[m]	n.d.	n.d.	n.d.	n.d.	n.d.	6.93	2.7	9.2	390	-69[b]
20				9.43[k,m]	n.d.	n.d.	2.76[k]	6.67[k]	n.d.	n.d.	9.27[m]	3.78[m]	n.d.	n.d.	n.d.	n.d.	n.d.	7.50	4.3	7.7	560	-30[b]
25				6.05[k,m]	n.d.	n.d.	2.77[k]	5.66[k]	n.d.	n.d.	6.36[m]	0.86[m]	n.d.	n.d.	n.d.	n.d.	n.d.	6.33	1.8	8.6	1180	-7[b]
32				5.94[k,m]	n.d.	n.d.	2.77[k]	5.58[k]	n.d.	n.d.	5.99[m]	0.86[m]	n.d.	n.d.	n.d.	n.d.	n.d.	5.99	1.6	8.6	1100	-65[b]
ave.				6.64	9.35	4.37	3.30	5.54	2.99	9.33	6.63	1.47	11.98	8.70	4.35	3.79	8.11	5.79				

[a] Effect on basal adenylate cyclase activity relative to potencies of methiothepin (−100% at 1.0×10^{-5} M. [b] Ligand concentration 1.0×10^{-4} M. [c] Ligand concentration 3.0×10^{-5} M. [d] Ligand concentration 1.0×10^{-5} M. [f] HYD3 is methyl substituent of piperidine ring. [h] HYD4 is centroid of cyclohexyl ring. [k] HYD1 is centroid of ring fused with six-membered aromatic ring of core. [m] HYD2 is middle between two *N*-methyl substituents. [n] Affinities and efficacies reported in the literature.[25,28] Not determined is abbreviated as n.d.

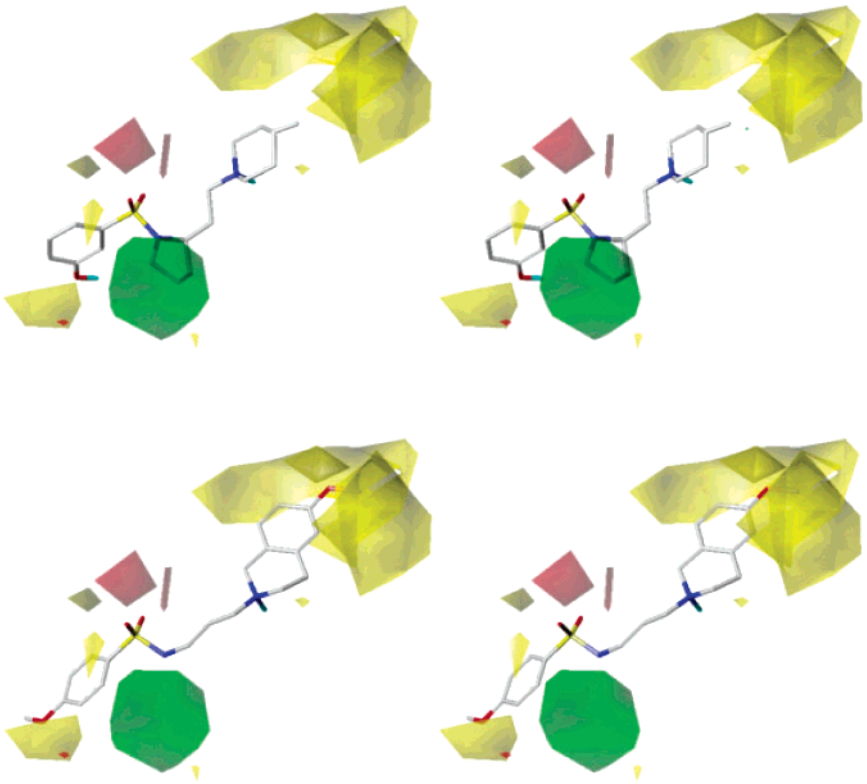

Figure 2. Stereo pictures of ligand **1b** (upper panel) and **14e** (lower panel) surrounded by CoMFA fields. Nonessential hydrogen atoms have been omitted.

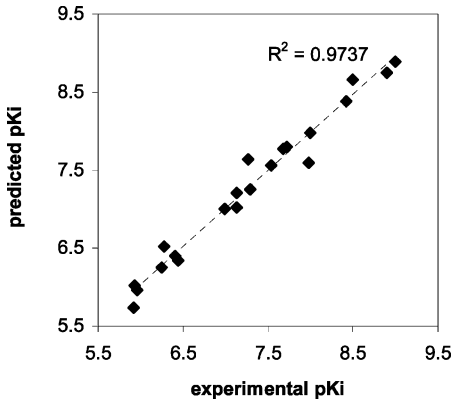

Figure 3. Correlation between actual and predicted pK_i values based on CoMFA computations.

Table 2. Partial Least Squares CoMFA Calculations

cross-validated run no. (two groups)	R^2	optimum no. components	mean SE of predictions
1	0.64	4	0.60
2	0.59	3	0.66
3	0.61	4	0.62
4	0.63	3	0.63
non-cross-validated run 1	0.97	6	0.18

Additional stabilizing interactions are contributed to Phe248 of TM5 (Phe$^{5.47}$) by means of $\pi-\pi$ stacking with the six-membered aromatic ring of 5-HT$_7$ receptor inverse agonists. Similar stabilizing interactions can be identified between Phe369 of TM7 (Phe$^{7.38}$) and the six-membered aromatic rings of THIQ and 2-methoxyphenyl piperazine moieties of the inverse agonists. In case of **1b**, it is suggested that C−H$\cdots\pi$ interactions between Phe$^{7.38}$ and the piperidine ring plays a supplementary role in receptor−ligand complex stabilization. This type of interaction is known for its significant role in stabilizing local structures of proteins as well.[42] Ligands **19**, **20**, **25**, and **32** that miss an aromatic ring similar to the arylsulfonamides and therefore are unable to form stabilizing interactions with Phe$^{5.47}$, show poor binding affinities. The shortage of this type of interactions with the binding site of the receptor is even more pronounced as a result of the absence of lipophilic substituents oriented near HYD2 and HYD3 of the pharmacophore model. Although **20** possesses a benzyl group that could achieve $\pi-\pi$ stacking interactions with Phe$^{7.38}$, the orientation of this group is far from optimal due to the conformations of the tetrahydropyridine ring structure (Figure 1), resulting in serious repulsive interactions with the boundaries of the lipophilic pocket instead.

In line with the results of this study, it is hypothesized that the pharmacophore for 5-HT$_7$ receptor inverse agonism consists of four hydrophobic domains (HYD1−4) instead of the three domains recently proposed by Lopez-Rodriguez et al in the model for 5-HT$_7$ receptor antagonism.[27] The fourth hydrophobic domain can host the aromatic ring of the arylsulfonamide moiety present in many inverse agonists (Chart 1). The dimensions of the extended pharmacophore model for 5-HT$_7$ receptor inverse agonism are listed in Table 1 and graphically illustrated in Figure 6.

Comparison of the currently extended pharmacophore model for 5-HT$_7$ receptor inverse agonism and the recently published pharmacophore model for 5-HT$_7$ receptor agonism[47] reveals a number of interesting similarities. The latter model (Figure 6, right panel) consists of a hydrophobic domain hosting the six-membered aromatic rings of indoles, 2-aminotetralins, and ergolines (HYD1), a region hosting a H-bond-

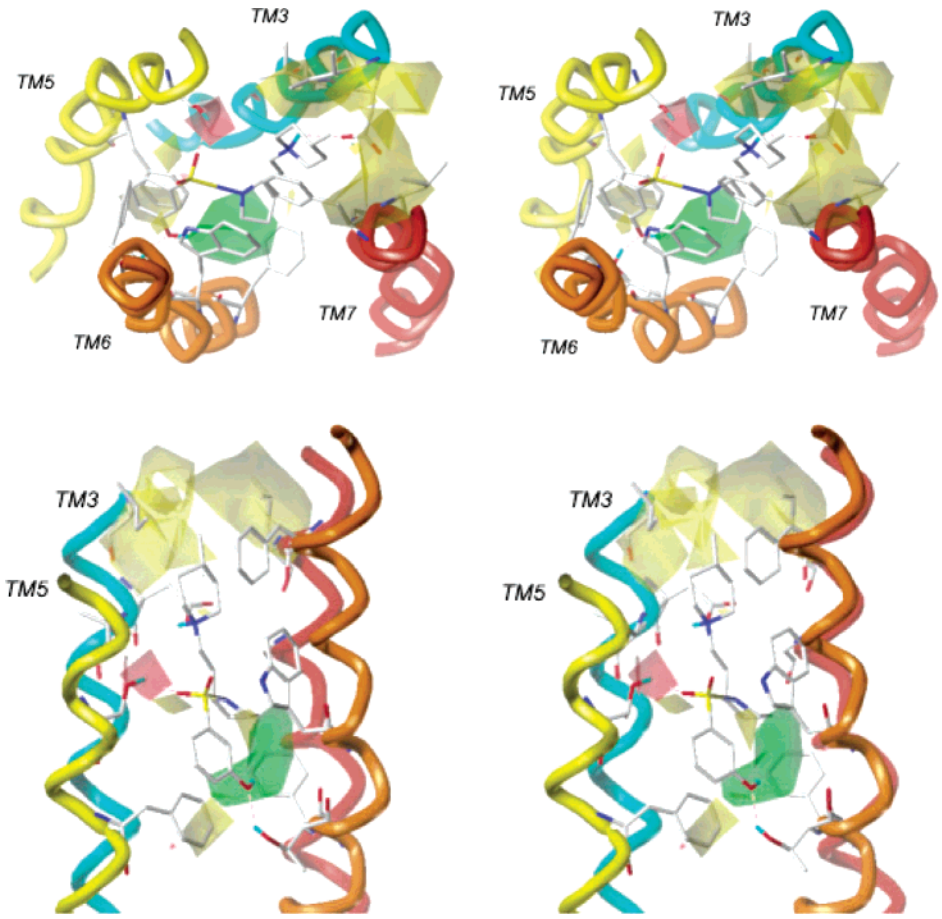

Figure 4. Stereoviews of CoMFA projections onto binding site of 5-HT$_7$ receptor with **1b** as an example. Top view (upper panel) and site view (lower panel). Nonessential hydrogen atoms have been omitted.

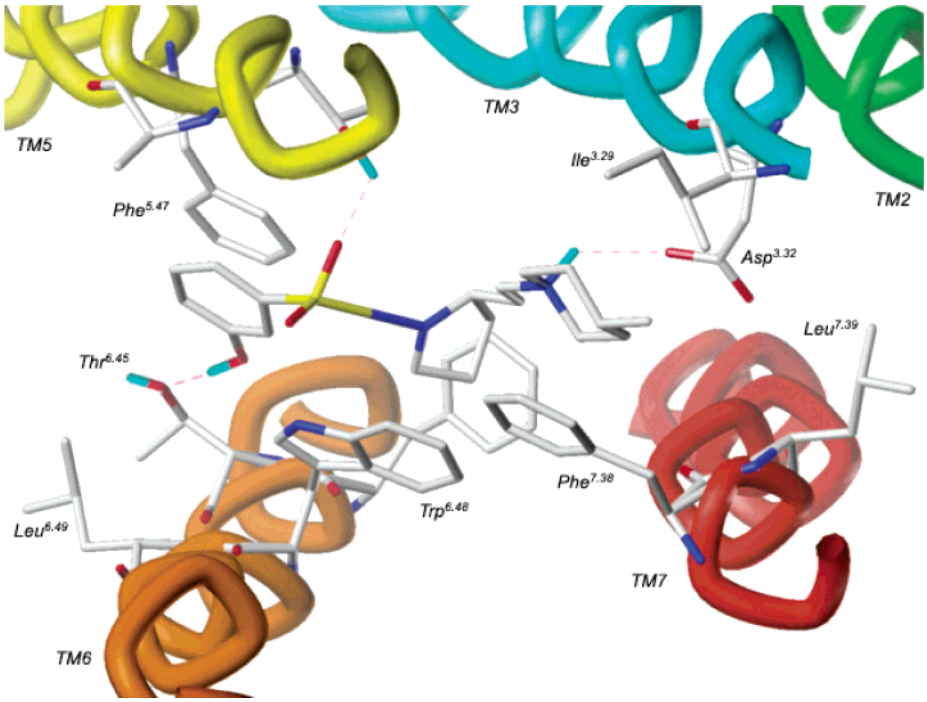

Figure 5. Close-up of molecular interactions between **1b** and binding site of 5-HT$_7$ receptor. Nonessential hydrogen atoms have been omitted.

donating (positively charged) nitrogen atom (PI), and a H-bond-accepting domain (HBA). SAR studies additionally revealed an extra hydrophobic domain (HYD2) for ligands that have an aromatic substituent instead of a substituent capable of accepting a H-bond from the hypothesized binding site residue. The dimensions of both models turn out to be very similar. While even the distance between HYD1 and HYD2 of the pharmaco-

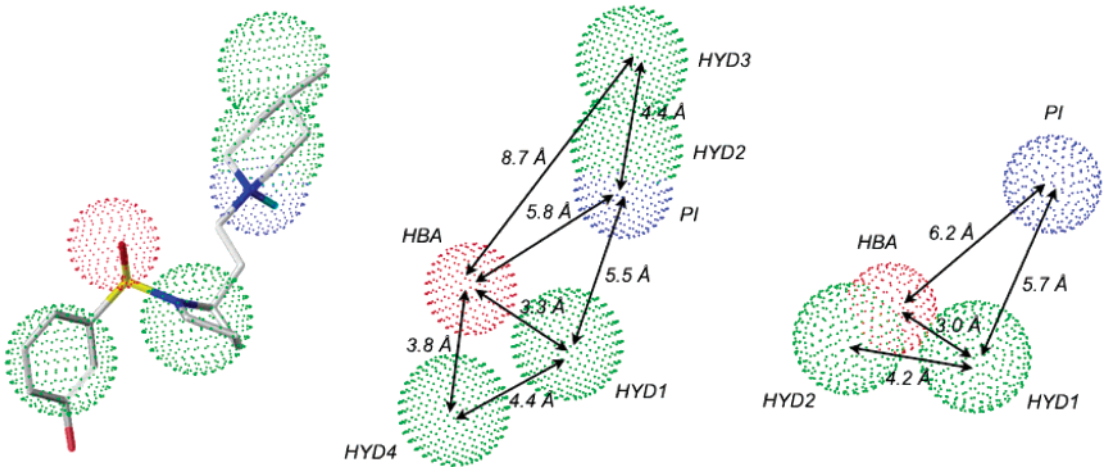

Figure 6. Pharmacophore models for 5-HT$_7$ receptor inverse agonism (middle panel) and 5-HT$_7$ receptor agonism (right panel). Ligand **1b** with projection of pharmacophore model for inverse agonism (left panel). Nonessential hydrogen atoms have been omitted.

phore model for agonism on one hand, and the corresponding distance between HYD1 and HYD4 of the pharmacophore model for inverse agonism, are nearly identical, the main difference between both models appears to be the presence of the additional HYD2 and HYD3 in the model for inverse agonism. This observation indirectly hints of the possibility of converting agonists into inverse agonists by connection of the protonatable nitrogen atom with substituents that can occupy these hydrophobic domains. Likewise, it was hypothesized that occupation of both the domains HBA and HYD2 of the pharmacophore model for 5-HT$_7$ receptor agonism could result in ligands with enhanced receptor affinity as well, compared to agonists occupying only either one of these domains. On the contrary, simultaneous occupation of these domains could also be (part of) the condition for 5-HT$_7$ receptor inverse agonism, since the majority of the ligands of the current set of 22 ligands demonstrate this simultaneous occupation of the corresponding domains HBA and HYD4 of the pharmacophore model for 5-HT$_7$ receptor inverse agonism.

The exact mechanism of action of ligands interacting with the 5-HT$_7$ receptor remains yet unrevealed. The residues Asp162 (Asp$^{3.32}$) and Thr244 (Thr$^{5.43}$) are important elements in binding the ligands to this site, but the presence of additional substituents appears to be conclusive with respect to the mode of action. It was demonstrated that both 5-HT$_7$ receptor agonists and inverse agonists show interactions with aromatic residues of TM6 (Phe$^{6.44}$, Trp$^{6.48}$, Phe$^{6.51}$, and Phe$^{6.52}$). In case of the dopamine D$_2$[16] and the 5-HT$_{2A}$ receptor,[38] it has been hypothesized that this cluster plays an important role in the mechanism of activation. Molecular interactions between a ligand, and this cluster would cause a conformational change at the so-called proline kink, effectuating TM6 to bend and giving the opportunity for TM6 and TM3 to move apart. Since this cluster of residues is highly conserved throughout the family of GPCRs, it is very likely that such a conformational change also plays a role in activation of the 5-HT$_7$ receptor by agonists and deactivation by inverse agonists.

Conclusion

The synthesis and pharmacological evaluation of a comprehensive set of novel inverse agonists has offered additional information in the process of characterization of the 5-HT$_7$ receptor. Especially the *N*-ethyl-substituted sulfonamides **13b**, **14b**, **14d**, **14f**, and **14h** appeared to be potent inhibitors of basal adenylate cyclase activity. Computational studies on the basis of these novel inverse agonists and a selection of previously published ligands resulted in a CoMFA model with a good correlation between experimental and predicted pK_i values, and a pharmacophore model that shows similarities with recently published pharmacophore models for 5-HT$_7$ receptor agonism and antagonism. In case of the 5-HT$_7$ receptor, there are reasonable indications that agonists and inverse agonists occupy the same binding site, but additional pharmacophoric features give rise to different conformational changes of the receptor resulting in activation by agonists and deactivation by inverse agonists.

Experimental Section

Molecular Computations. Conformational Analysis. Calculations of physical properties (log *P*, pK_a) were performed with Pallas.[1] All molecular computations were performed on a Silicon Graphics O2 workstation running IRIX 6.3 or a Silicon Graphics IRIS Indigo XS/4000 workstation running IRIX 5.3. For conformational analyses, ligands were sketched with the correct stereochemistry, if present, in their protonated, positively charged state from standard fragments in MacroModel.[2] Structures were minimized with default options prior to full conformational analysis. Conformational analyses were performed using the Monte Carlo Multiple Minimum (MCMM) search protocol[10] with a minimum of 1500 steps via the SUMM option.[14] Minimizations were performed using the Truncated Newton Conjugate Gradient (TNCG) minimization method within the MM2 force field[4,23,24] with simulation of a distance dependent water continuum[43] as implemented in MacroModel. Per step, 250 iterations were performed until the gradient reached the value of 0.01 kcal Å^{-1} mol^{-1}. All conformations within a range of 50 kJ/mol above the global minimum were considered to be relevant. In case of nonchiral ligands, mirror images were preserved using the NANT option. Additional information needed for subsequent calculations with the pharmacophore identifying software program APOLLO was obtained through incorporation of DEBG options 3 and 28. Torsion bonds of *n*-propyl chains were fixed in their anti-

staggered conformation to reduce the number of low energy conformations. Molecular dimensions and atomic distances were determined by manual selection of the appropriate atomic features in the Analyze mode.

Pharmacophore Identification. The VECADD module of APOLLO[40] was used to define extension vectors and centroids to all low energy conformations of all ligands as calculated by MacroModel in the previously described section. Extension vectors were allocated to the lone-pairs of the oxygen atoms of substituents (if present) of the six-membered aromatic ring present in all ligands, and the protonated, positively charged nitrogen atom also present in all ligands. The RMSFIT module of APOLLO subsequently identified the conformations of the ligands that exhibited the best overall least-squares fit with respect to the specified extension vectors and centroids. This calculation was performed in an energy dependent manor, while all fitting points were considered equally important. In case multiple solutions were calculated, the matches were ranked with respect to conformational energies and root-mean-square deviations. The best fit was extracted from the RMSFIT output file using the MMDFIT module of APOLLO.

CoMFA Computations. Selected conformations of the ligands were imported into a Sybyl[3] database as pdb-files as selected by the APOLLO molecular modeling and extracted from the RMSFIT output file using the MMDFIT module. Atom types were checked and adjusted if necessary, extension vectors and centroids were deleted, and atomic charges were calculated (Gasteiger−Hückel). On the basis of these database, a new MSS was opened, and pK_i values were entered manually. CoMFA parameters calculated with Sybyl standard parameters and with steric and dielectric cutoff values of 15 and 10 kcal/mol, respectively (distance dependent dielectric function), were inserted as separate column. Partial least squares (PLS) calculations (non-cross-validated) resulted in the described CoMFA model, which was subsequently used for mapping onto the binding site of the 5-HT_7 receptor to identify conceivable amino acid residues.

Homology Modeling of the Receptor. The sequence of 449 amino acids of the human 5-HT_{7A} receptor was taken from the SwissProt database (entry P34969; http://us.expasy.org/sprot/). On the basis of the identification of evolutionary highly conserved amino acids within the rhodopsin-based family of G-protein-coupled receptors, the helical parts of the receptor were manually aligned with a template of α-carbon atoms of the transmembrane domains.[5] Initial minimization of the helices separately (Tripos force field, Gasteiger−Hückel charges, dielectric constant 5.0, distance dependent, conjugate gradient 0.1 kcal/mol/Å), and subsequent minimization of the ensemble of the 7 transmembrane helices resulted in the model with a total energetic value lower than the sum of energies of the individually minimized helices.

Mapping of CoMFA Model onto Receptor Binding Site. The CoMFA model was projected onto the binding site to identify conceivable amino acid residues that could account for the contour maps as computed during the comparative molecular field analysis. For this purpose, the three-dimensional orientation of mutual interaction points, as calculated from the preceding alignment procedure by APOLLO, were used to locate the ligand binding amino acid residues in the receptor binding site. The mutual interaction point forming H-bonds with the HBA moieties of the ligands was superimposed onto Thr244 ($Thr^{5.43}$), and the H-bond-accepting interaction point forming H-bonds with the PI moieties of the ligands was superimposed onto Asp162 ($Asp^{3.32}$).

Docking of Ligands in Binding Site. Ligands were manually docked into the binding site as described and minimized to analyze the ligand binding interactions. This docking procedure was guided by mapping the mutual interaction points as calculated from the preceding alignment procedure by APOLLO onto the previously mentioned amino acid residues. As a starting point for minimization, the conformations of the ligands used for superpositioning in APOLLO were used, and the side chains of the hypothesized amino acid residues were adjusted, if necessary, to adopt the three-dimensional orientation of mutual interaction points in the most optimal manor. Minimization of the merged complex of ligand and receptor (Tripos force field, Gasteiger−Hückel charges, NB cutoff 8.0, dielectric constant 5.0, distance dependent, conjugate gradient 0.1 kcal/mol/Å) resulted in properly docked ligands.

Chemistry. General Remarks. The purity of the target compounds was established using multiple techniques. IR spectra were recorded on an ATI-Mattson Genesis Series FT-IR spectrophotometer. NMR data were recorded using Varian Gemini-200 and Varian VXR-300 spectrometers (^{1}H NMR at 200 or 300 MHz, ^{13}C NMR at 50 or 75 MHz). Chemical shifts are denoted in δ units (ppm) relative to the solvent (^{1}H NMR peaks: 7.26 for $CDCl_3$ and 3.30 for CD_3OD. ^{13}C NMR peaks: 76.91 for $CDCl_3$ and 49.50 for CD_3OD). Electron impact (EI^+) mass spectra were recorded on a Unicam Automass mass spectrometer in conjunction with a gas chromatograph. TLC analyses were carried out on aluminum plates (Merck) precoated with silica gel 60 F_{254} (0.2 mm). Visualization of spots was performed with UV light and a commonly used alkaline $KMnO_4$ spray solution or Silica coated I_2. Elemental analyses (C, H, N) of target compounds were performed at the University of Groningen.

[4-(2-Methoxyphenyl)piperazin-1-yl]acetonitrile (6). 2-Methoxyphenylpiperazin hydrochloride (0.23 g, 1.00 mmol) was suspended in acetonitrile under nitrogen atmosphere. Bromoacetonitrile (0.14 g, 1.10 mmol) and K_2CO_3 (0.35 g, 2.50 mmol) were added, followed by the addition of KI (cat. amount) and DMF (1 drop). The mixture was heated to a gentle reflux overnight. The cooled suspension was filtered and concentrated in vacuo. The residue was partioned between CH_2Cl_2 (30 mL) and water (10 mL). The organic layer was subsequently dried (Na_2SO_4), filtered, and concentrated to yield a brown oil (0.23 g, 99% yield) that was purified by chromatography (Silica, CH_2Cl_2/CH_3OH, 19:1). ^{1}H NMR (300 MHz, $CDCl_3$) δ (ppm): 2.74 (t, J = 4.8 Hz, 4H), 3.07 (br, 4H), 3.49 (s, 2H), 3.80 (s, 3H), 6.80−6.87 (m, 3H), 6.93−6.97 (m, 1H). ^{13}C NMR (75 MHz, $CDCl_3$) δ (ppm): 43.5, 47.7, 49.6, 53.0, 108.9, 112.4, 115.8, 118.5, 120.7, 138.3, 149.8. IR (neat, cm^{-1}): 2940, 2826, 2231, 1675, 1593, 1501, 1452, 1382, 1302, 1239, 1140, 1012, 927, 861, 751. MS (EI^+): 231, 191, 136, 92, 56 (100%).

3-[4-(2-Methoxyphenyl)piperazin-1-yl]propionitrile (7). 2-Methoxyphenylpiperazine (0.55 g, 2.86 mmol) was dissolved in ethanol (10 mL) and acrylonitrile (0.50 g, 9.40 mmol). The mixture was heated to reflux for 1 h. The volatiles were removed under reduced pressure to yield the crude product as colorless crystals (0.64 g, 97% yield). ^{1}H NMR (300 MHz, $CDCl_3$) δ (ppm): 2.50 (t, J = 7.0 Hz, 2H), 2.64−2.75 (m, 6H), 3.05 (br, 4H), 3.81 (s, 3H), 6.80−6.98 (m, 4H). ^{13}C NMR (75 MHz, $CDCl_3$) δ (ppm): 13.3, 48.0, 50.4, 51.0, 52.8, 108.7, 115.7, 118.5, 120.6, 148.5. IR (neat, cm^{-1}): 2945, 2829, 2249, 1591, 1501, 1449, 1239, 1141, 1024, 935, 751. MS (EI^+): 245, 205, 177, 120, 70 (100%). Mp (uncorrected): 83 °C.

2-[4-(2-Methoxyphenyl)piperazin-1-yl]ethylamine (9). Nitrile **6** (0.23 g, 1.00 mmol) was dissolved in THF (dry, 10 mL) and added dropwise to a freshly prepared suspension of $LiAlH_4$ (0.08 g, 2.10 mmol) in THF (dry, 10 mL) under nitrogen atmosphere. The mixture was stirred at room temperature for 1 h. Careful workup by subsequent addition of water (1 equiv), NaOH (1 N, 1 equiv) and water (4 equiv). Na_2SO_4 was added and the suspension was then filtered over Celite. The clear solution was concentrated in vacuo. The oil thus obtained (0.19 g, 81% yield) was used without further purification. ^{1}H NMR (300 MHz, $CDCl_3$) δ (ppm): 1.41 (br, 2H), 2.40 (t, J = 5.9 Hz, 2H), 2.56 (br, 4H), 2.73 (br, 2H), 3.00 (br, 4H), 3.75 (s, 3H), 6.75−6.93 (m, 4H). ^{13}C NMR (75 MHz, $CDCl_3$) δ (ppm): 48.2, 51.0, 52.8, 58.7, 108.6, 115.6, 118.4, 120.3, 138.8, 149.7. IR (neat, cm^{-1}): 2939, 2816, 1590, 1498, 1450, 1240, 1145, 1030, 749. MS (m/z): 236 (M + 1).

3-[4-(2-Methoxyphenyl)piperazin-1-yl]propylamine (10a). The nitrile ***7*** (0.24 g, 1.00 mmol) was dissolved in diethyl ether (dry, 10 mL) and added dropwise to a freshly prepared suspension of $AlCl_3$ (0.27 g, 2.00 mmol) and $LiAlH_4$ (0.08 g, 2.10 mmol) in diethyl ether (dry, 15 mL) under nitrogen

atmosphere. The mixture was allowed to stir at room temperature for 1 h. Careful addition of water decomposed the excess of reactants. NaOH (50 mL, 0.5 N) was added and extracted with CH_2Cl_2 (4 × 20 mL). The combined organic layers were dried (Na_2SO_4), filtered, and concentrated in vacuo to yield **10a** as a colorless oil (0.21 g, 84% yield) which was used without further purification. ^{1}H NMR (300 MHz, $CDCl_3$) δ (ppm): 1.35 (br, 2H), 1.54 (t, J = 7.0 Hz, 2H), 2.33−2.38 (m, 2H), 2.54 (br, 4H), 2.62−2.66 (m, 2H), 2.98 (br, 4H), 3.73 (s, 3H), 6.71 (d, J = 7.7 Hz, 1H), 6.77−6.89 (m, 3H). ^{13}C NMR (75 MHz, $CDCl_3$) δ (ppm): 28.0, 38.3, 48.1, 51.0, 52.8, 54.1, 108.6, 115.6, 118.4, 120.3, 138.8, 149.7. IR (neat, cm^{-1}): 3365, 3286, 2938, 2814, 1593, 1500, 1451, 1376, 1301, 1240, 1144, 1028, 927, 748. MS (m/z): 250 (M + 1).

Method A: preparation of acetamides **10b** and **11b**, and sulfonamides **12**, **13a**−**c**, and **14a**−**h**: Primary amines were dissolved in a vigorously stirred mixture of CH_2Cl_2 (generally 20 mL) and $NaHCO_3$ (sat. solution, generally 10 mL). After addition of the acetic anhydride or arylsulfonyl chloride, stirring was applied for 30−300 min at room temperature. Then, the layers were separated and the water layer was washed with CH_2Cl_2. The combined organic layers were dried (Na_2SO_4) and filtered. Evaporation of the volatiles yielded the crude products.

***N*-{3-[4-(2-Methoxyphenyl)piperazin-1-yl]propyl}-acetamide (10b).** Method A was applied, using crude **10a** (0.16 g, 0.65 mmol) and acetic anhydride (0.10 g, 1.00 mmol). This yielded crude **10b** (0.18 g, 95% yield) as a slightly yellow oil that crystallized upon standing. ^{1}H NMR (300 MHz, $CDCl_3$) δ (ppm): 1.66 (dt, J = 6.2 Hz, 2H), 1.90 (s, 3H), 2.14 (br, 1H), 2.50 (t, J = 6.2 Hz, 2H), 2.63 (br, 4H), 3.04 (br, 4H), 3.28−3.34 (m, 2H), 3.81 (s, 3H), 6.81 (d, J = 7.7 Hz, 1H), 6.86−6.88 (m, 1H), 6.90−6.99 (m, 1H), 7.15 (br, 1H). ^{13}C NMR (75 MHz, $CDCl_3$) δ (ppm): 21.0, 22.4, 37.3, 48.3, 50.9, 52.9, 55.2, 108.7, 115.6, 118.5, 120.6, 138.5, 149.7, 167.3. IR (neat, cm^{-1}): 3303, 2946, 2812, 1639, 1562, 1501, 1438, 1376, 1303, 1240, 1145, 1026, 743. MS (m/z): 292 (M + 1).

***N*-{2-[4-(2-Methoxyphenyl)piperazin-1-yl]ethyl}-4-methylbenzenesulfonamide (12).** Method A was applied, using **9** (0.19 g, 0.80 mmol) and *p*-toluenesulfonyl chloride (0.17 g, 0.90 mmol). This yielded a yellow oil (0.27 g, 87% yield) that was purified by chromatography (Silica, CH_2Cl_2/CH_3OH, 99:1) to yield pure **12** as oil. The free base was converted to its oxalate salt by treatment with oxalic acid dihydrate in ethanol. Recrystallization form ethanol yielded the pure compound. ^{1}H NMR (free base, 300 MHz, $CDCl_3$) δ (ppm): 2.42−2.50 (m, 9H), 3.03−3.10 (m, 6H), 3.84 (s, 3H), 5.28 (br, 1H), 6.84−7.04 (m, 4H), 7.32 (d, J = 8.6 Hz, 2H), 7.78 (d, J = 8.3 Hz, 2H). ^{13}C NMR (75 MHz, $CDCl_3$) δ (ppm): 20.1, 37.8, 49.0, 51.2, 53.9, 54.2, 109.7, 116.7, 119.5, 121.6, 125.7, 128.2, 135.1, 139.6, 141.9, 150.7. IR (neat, cm^{-1}): 3300, 2954, 2810, 1596, 1499, 1449, 1326, 1235, 1154, 1091, 1024, 834, 747. MS (EI$^+$): 389, 205 (100%), 190, 162, 120, 92, 70. Mp (uncorrected): 162−164 °C. Anal. ($C_{20}H_{27}N_3O_3S\_C_2H_2O_4$) C, H, N.

***N*-{3-[4-(2-Methoxyphenyl)piperazin-1-yl]propyl}-4-methylbenzenesulfonamide (13a).** Method A was applied, using **10a** (0.12 g, 0.48 mmol) and *p*-toluenesulfonyl chloride (0.11 g, 0.60 mmol). This yielded a yellow oil (0.19 g, 98% yield) that was purified by chromatography (Silica, CH_2Cl_2/CH_3OH, 98:2) to yield pure **13a** as oil. The free base was converted to its oxalate salt by treatment with oxalic acid dihydrate in ethanol. ^{1}H NMR (free base, 300 MHz, $CDCl_3$) δ (ppm): 1.55−1.60 (m, 2H), 2.34 (s, 3H), 2.37−2.40 (t, J = 5.9 Hz, 3H), 3.53 (br, 4H), 2.99−3.02 (m, 6H), 3.78 (s, 3H), 6.79 (d, J = 7.7 Hz, 1H), 6.83−6.96 (m, 3H), 7.22 (d, J = 8.1 Hz, 2H), 7.67 (d, J = 8.1 Hz, 2H). ^{13}C NMR (75 MHz, $CDCl_3$) δ (ppm): 19.0, 21.5, 41.7, 48.2, 50.8, 52.9, 55.5, 108.7, 115.9, 118.5, 120.6, 124.5, 127.1, 134.7, 138.4, 140.5, 149.7. IR (neat, cm^{-1}): 3302, 2940, 2805, 1592, 1496, 1449, 1325, 1244, 1150, 1091, 1022, 827, 746. MS (EI$^+$): 403, 388, 205, 177, 136, 91 (100%), 56. Mp (uncorrected): 171−173 °C. Anal. ($C_{21}H_{29}N_3O_3S\cdot C_2H_2O_4$) C, H, N.

***N*-Ethyl-*N*-{3-[4-(2-methoxyphenyl)piperazin-1-yl]propyl}-4-methylbenzenesulfonamide (13b).** Acetamide **10b** (0.08 g, 0.26 mmol) was dissolved in THF (dry, 5 mL) and added dropwise to a freshly prepared suspension of $LiAlH_4$ (0.02 g, 0.53 mmol) in THF (dry, 5 mL) under nitrogen atmosphere. The mixture was warmed to reflux for 2 h. Excess of reactant was decomposed by addition of water (25 mL). The water layer was extracted with CH_2Cl_2 (3 × 10 mL), and the combined organic layers were dried over Na_2SO_4 and filtered. Evaporation of volatiles yielded the intermediate amine **10c** as colorless oil (0.08 g, 99% yield). MS (EI$^+$): 277, 262, 219, 190, 162, 120, 70, 58 (100%). The oil was dissolved in CH_2Cl_2 (5 mL), and *p*-toluenesulfonyl chloride (0.10 g, 0.53 mmol) was added. $NaHCO_3$ (5 mL, sat) was added, and the mixture was stirred vigorously for 4 h at room temperature. The layers were separated, and the water layer was washed with CH_2Cl_2 (5 mL). The combined organic layers were dried (Na_2SO_4), filtered, and concentrated in vacuo. This yielded an oil that was purified by chromatography (Silica, CH_2Cl_2/CH_3OH, 98:2) to yield pure **13b** as an oil (0.09, 80% yield). The free base was converted to its oxalate salt by treatment with oxalic acid dihydrate in ethanol. ^{1}H NMR (free base, 300 MHz, $CDCl_3$) δ (ppm): 1.03−1.08 (t, J = 7.0 Hz, 3H), 1.74 (dt, J = 7.3 Hz, 2H), 2.33−2.38 (m, 5H), 2.56 (br, 4H), 3.02 (br, 4H), 3.11−3.21 (m, 4H), 3.80 (s, 3H), 6.80 (d, J = 8.1 Hz, 1H), 6.85−6.96 (m, 3H), 7.23 (d, J = 8.1 Hz, 2H), 7.64 (d, J = 8.1 Hz, 2H). ^{13}C NMR (75 MHz, $CDCl_3$) δ (ppm): 11.5, 19.0, 23.8, 40.4, 43.2, 48.1, 50.9, 52.8, 53.1, 108.7, 115.6, 118.5, 120.4, 124.6, 127.1, 134.6, 138.8, 140.5, 149.7. IR (neat, cm^{-1}): 3280, 2948, 2818, 1598, 1500, 1450, 1328, 1239, 1154, 1092, 1025, 830, 752.MS (EI$^+$): 431, 276, 205 (100%), 155, 120, 91 (100%), 56. Mp (uncorrected): 178−180 °C. Anal. ($C_{23}H_{33}N_3O_3S\cdot C_2H_2O_4$) C, H, N.

4-Methoxy-*N*-{3-[4-(2-methoxyphenyl)piperazin-1-yl]-propyl}-benzenesulfonamide (13c). Method A was applied, using **10a** (0.05 g, 0.20 mmol) and *p*-toluenesulfonyl chloride (0.08 g, 0.35 mmol). This yielded an oil (0.07 g, 83% yield) that was purified by chromatography (Silica, CH_2Cl_2/CH_3OH, 99:1) to yield pure **13c** as oil. The free base was converted to its oxalate salt by treatment with oxalic acid dihydrate in ethanol. ^{1}H NMR (free base, 300 MHz, $CDCl_3$) δ (ppm): 1.19 (br, 1H), 1.60 (dt, J = 5.5 Hz, 2H), 2.40 (t, J = 5.9 Hz, 2H), 2.54 (br, 4H), 3.01 (t, J = 5.9 Hz, 6H), 3.79 (s, 6H), 6.79 (d, J = 7.7 Hz, 1H), 6.86−6.95 (m, 5H), 7.73 (d, J = 7.0 Hz, 2H). ^{13}C NMR (75 MHz, $CDCl_3$) δ (ppm): 21.5, 41.7, 48.2, 50.8, 52.9, 53.1, 55.6, 108.6, 111.6, 115.9, 118.5, 120.6, 126.5, 129.4, 138.4, 149.7, 160.1. IR (neat, cm^{-1}): 3281, 2944, 2820, 1596, 1499, 1454, 1327, 1241, 1155, 1095, 1026, 834, 749. MS (EI$^+$): 419, 404, 205, 171, 140, 107, 77 (100%). Mp (uncorrected): 183−186 °C. Anal. ($C_{21}H_{29}N_3O_4S\cdot C_2H_2O_4$) C, H, N.

3-(6-Methoxy-3,4-dihydro-1*H*-isoquinolin-2-yl)propionitrile (8). 6-Methoxy-1,2,3,4-tetrahydroisoquinoline hydrochloride (**5**,[11] 5.00 g, 25.1 mmol) was dissolved in ethanol (100 mL) and treated with triethylamine (2.54 g, 25.1 mmol) and an access of acrylonitrile (4.00 g, 75.4 mmol). The mixture was heated to reflux for 5 h. The volatiles were removed under reduced pressure, and the residue was partioned between CH_2Cl_2 and water. The organic layer was washed with brine, dried (Na_2SO_4), and filtered. Evaporation of the solvent yielded the crude product, which could be purified by chromatography (Silica, CH_2Cl_2/CH_3OH, 99:1) to yield pure **8** as a slightly yellow oil (5.21 g, 96% yield). ^{1}H NMR (200 MHz, $CDCl_3$) δ (ppm): 0.99 (m, 1H), 1.26 (s, 1H), 1.43 (s, 1H), 1.63−1.82 (m, 1H), 2.59 (t, J = 6.8 Hz, 2H), 2.66−2.79 (m, 2H), 2.87 (s, 1H), 3.57 (s, 1H), 3.76 (s, 3H), 6.60−6.70 (m, 2H), 6.91−6.98 (m, 1H). ^{13}C NMR (50 MHz, $CDCl_3$) δ (ppm): 28.2, 28.8, 39.3, 49.3, 53.7, 54.2, 55.1, 110.6, 111.6, 124.0, 126.0, 133.8, 156.5. IR (neat, cm^{-1}): 2930, 2834, 2247, 1610, 1506, 1272, 1146, 1037, 811. MS (m/z): 217 (M + 1).

3-(6-Methoxy-3,4-dihydro-1*H*-isoquinolin-2-yl)propylamine (11a). ***8*** (3.70 g, 17.1 mmol) was dissolved in THF (dry, 10 mL) and added dropwise to a freshly prepared suspension of $AlCl_3$ (4.10 g, 30.8 mmol) and $LiAlH_4$ (1.20 g, 31.6 mmol) in THF (dry, 250 mL) under nitrogen atmosphere. The mixture was allowed to stir at room temperature overnight. Workup was initiated by careful subsequent addition of water (1 equiv),

NaOH (1 N, 1 equiv), and water (4 equiv) and filtration of the salts thus formed over Celite. The clear solution was dried (Na_2SO_4) and concentrated in vacuo. This yielded **11a** as a yellow-green oil (3.24 g, 86% yield), which was used for further reactions without purification. ^{1}H NMR (200 MHz, $CDCl_3$) δ (ppm): 2.63 (t, J = 6.3 Hz, 2H), 2.75−3.00 (m, 10 H), 3.66 (s, 2H), 3.81 (s, 3H), 6.81 (m, 3H). ^{13}C NMR (50 MHz, $CDCl_3$) δ (ppm): 15.1, 27.7, 49.0, 51.4, 55.1, 55.3, 121.0, 121.9, 124.7, 126.7, 133.3, 156.6. IR (neat, cm^{-1}): 3359, 2930, 1612, 1505, 1271, 1138, 1038, 812. MS (*m*/*z*): 221 (M + 1).

***N*-[3-(6-Methoxy-3,4-dihydro-1*H*-isoquinolin-2-yl)propyl]acetamide (11b).** Method A was applied, using crude **11a** (2.30 g, 10.5 mmol) and acetic anhydride (1.44 g, 15.0 mmol). This yielded crude **11b** (2.49 g, 91% yield) as a slightly brown oil that was used without further purification. IR (neat, cm^{-1}): 3290, 2930, 1824, 1650, 1505, 1447, 1373, 1271, 1138, 1036, 904, 813. MS (*m*/*z*): 263 (M + 1).

Ethyl-[3-(6-methoxy-3,4-dihydro-1*H*-isoquinolin-2-yl)-propyl]amine (11c). 11b (crude, 2.49 g, ca. 9.5 mmol) was dissolved in THF (dry, 15 mL) and added dropwise to a freshly prepared suspension of $LiAlH_4$ (0.60 g, 15.8 mmol) in THF (dry, 75 mL) under nitrogen atmosphere. The mixture was refluxed overnight. Careful workup by subsequent addition of water (1 equiv), NaOH (1 N, 1 equiv) and water (4 equiv) and filtration of the salts thus formed over Celite yielded a clear solution that was dried (Na_2SO_4) and concentrated in vacuo. The oil thus obtained (2.54 g, 99% yield) was purified by chromatography (Silica, CH_2Cl_2/CH_3OH, 99:1). ^{1}H NMR (200 MHz, $CDCl_3$) δ (ppm): 0.96 (t, J = 6.4 Hz, 3H), 1.48−1.52 (m, 2H), 2.34−2.72 (m, 10 H), 3.24 (br, 1H), 3.60 (s, 2H), 3.76 (s, 3H), 6.62−6.74 (m, 2H), 6.92−6.98 (m, 1H). ^{13}C NMR (50 MHz, $CDCl_3$) δ (ppm): 15.8, 28.8, 30.0, 41.2, 45.4, 51.2, 54.8, 56.0, 110.8, 112.2, 130.5, 131.2, 138.9, 156.8. IR (neat, cm^{-1}): 2929, 1612, 1505, 1464, 1269, 1159, 1038, 803. MS (*m*/*z*): 249 (M + 1).

***N*-[3-(6-Methoxy-3,4-dihydro-1*H*-isoquinolin-2-yl)propyl]-benzenesulfonamide (14a).** Method A was applied, using benzenesulfonyl chloride (0.18 g, 1.02 mmol) and **11a** (0.20 g, 0.93 mmol). This yielded an oil that was purified by chromatography (Silica, CH_2Cl_2/CH_3OH, 19:1) to yield pure **14a** (0.27 g, 81% yield). The free base was converted to its hydrochloric salt by treatment with HCl (1 N solution in diethyl ether). ^{1}H NMR (free base, 200 MHz, $CDCl_3$) δ (ppm): 0.80−0.99 (m, 1H), 1.30 (s, 1H), 1.72 (s, 1H), 1.93−2.10 (m, 1H), 2.52 (t, J = 6.8 Hz, 2H), 2.65 (t, J = 5.8 Hz, 2H), 2.90 (t, J = 6.0 Hz, 2H), 2.99 (t, J = 6.0 Hz, 2H), 3.72 (s, 3H), 6.60−6.77 (m, 2H), 6.97 (d, J = 8.5 Hz, 1H), 7.50−7.70 (m, 4H), 8.05 (d, J = 1.0 Hz, 1H). ^{13}C NMR (50 MHz, $CDCl_3$) δ (ppm): 27.9, 28.2, 42.1, 46.3, 48.9, 53.8, 54.0, 125.5, 126.0, 127.6, 132.1, 132.3, 138.4. IR (neat, cm^{-1}): 3411, 2937, 2485, 1614, 1509, 1448, 1371, 1167, 1084, 721, 551. MS (*m*/*z*): 361 (M + 1). Mp (uncorrected): 126−128 °C. Anal. ($C_{19}H_{24}N_2O_3S$·Cl) C, H, N.

***N*-Ethyl-*N*-[3-(6-methoxy-3,4-dihydro-1*H*-isoquinolin-2-yl)propyl]-benzenesulfonamide (14b).** Method A was applied, using benzenesulfonyl chloride (0.07 g, 0.36 mmol) and **11c** (0.05 g, 0.18 mmol). This yielded an oil that was purified by chromatography (Silica, CH_2Cl_2/CH_3OH, 19:1) to yield pure **14b** (0.05 g, 39% yield). The free base was converted to its oxalate salt by treatment with oxalic acid dihydrate in ethanol. ^{1}H NMR (free base, 200 MHz, $CDCl_3$) δ (ppm): 1.12 (t, J = 7.2 Hz, 2H), 1.31 (s, 1H), 1.85−1.92 (m, 4H), 2.58 (t, J = 7.2 Hz, 2H), 2.74 (t, J = 5.5 Hz, 2H), 2.89 (t, J = 5.6 Hz, 2H), 3.21−3.28 (q, J = 7.3 Hz, 3H), 3.56 (s, 1H), 3.78 (s, 3H), 6.64−6.74 (m, 2H), 6.94 (d, J = 8.6 Hz, 1H), 7.49−7.59 (m, 4H), 7.84 (d, J = 7.8 Hz, 1H). ^{13}C NMR (50 MHz, $CDCl_3$) δ (ppm): 12.5, 25.0, 27.6, 28.2, 44.3, 49.2, 53.6, 53.8, 110.7, 111.7, 124.8, 125.5, 126.6, 127.5, 130.8, 133.6, 138.5, 156.6. IR (neat, cm^{-1}): 2927, 1690, 1611,, 1505, 1335, 1159, 1036, 802, 692. MS (*m*/*z*): 389 (M + 1). Mp (uncorrected): 159−162 °C. Anal. ($C_{21}H_{28}N_2O_3S$·$C_2H_2O_4$) C, H, N.

***N*-[3-(6-Methoxy-3,4-dihydro-1*H*-isoquinolin-2-yl)propyl]-4-methylbenzenesulfonamide (14c).** Method A was applied, using **11a** (0.13 g, 0.59 mmol) and *p*-toluenesulfonyl chloride (0.12 g, 0.65 mmol). This yielded an oil (0.17 g, 77% yield) that was purified by chromatography (Silica, CH_2Cl_2/CH_3OH, 96:4) to yield pure **14c** as oil. The free base was converted to its oxalate salt by treatment with oxalic acid dihydrate in ethanol. ^{1}H NMR (free base, 200 MHz, $CDCl_3$) δ (ppm): 1.69−1.75 (m, 4H), 2.42 (s, 1H), 2.55 (t, J = 10.3 Hz, 2H), 2.69 (t, J = 5.7 Hz, 2H), 2.90 (t, J = 5.7 Hz, 2H), 3.09 (t, J = 5.9 Hz, 2H), 3.49 (s, 3H), 3.80 (s, 3H), 6.65−6.76 (m, 4H), 6.92 (d, J = 8.6 Hz, 1H), 7.26 (d, J = 8.3 Hz, 1H) 7.65 (d, J = 8.3 Hz, 1H). ^{13}C NMR (50 MHz, $CDCl_3$) δ (ppm): 20.0, 23.2, 27.6, 42.4, 48.7, 53.8, 54.4, 55.9, 110.9, 111.7, 124.6, 125.5, 125.8, 133.6, 135.7, 141.5, 158.6. IR (neat, cm^{-1}): 2932, 1612, 1505, 1455, 1328, 1159, 815. MS (*m*/*z*): 375 (M + 1). Mp (uncorrected): 158−160 °C. Anal. ($C_{20}H_{26}N_2O_3S$·$C_2H_2O_4$) C, H, N.

***N*-Ethyl-*N*-[3-(6-methoxy-3,4-dihydro-1*H*-isoquinolin-2-yl)propyl]-4-methylbenzenesulfonamide (14d).** Method A was applied, using **11c** (0.25 g, 1.35 mmol) and *p*-toluenesulfonyl chloride (0.11 g, 0.45 mmol). This yielded an oil (0.30 g, 55% yield) that was purified by chromatography (Silica, CH_2Cl_2/CH_3OH, 95:5) to yield pure **14d** as slightly yellow oil. The free base was converted to its oxalate salt by treatment with oxalic acid dihydrate in ethanol. ^{1}H NMR (free base, 200 MHz, $CDCl_3$) δ (ppm): 1.13 (t, J = 7.2 Hz, 2H), 1.82−1.90 (m, 5H), 2.42 (s, 1H), 2.53 (t, J = 7.2 Hz, 2H), 2.69 (t, J = 5.7 Hz, 2H), 2.88 (t, J = 5.7 Hz, 2H), 3.18−3.30 (q, J = 5.8 Hz, 3H), 3.54 (s, 3H), 3.78 (s, 3H), 6.64−6.73 (m, 4H), 7.29 (d, J = 5.6 Hz, 1H), 7.68 (d, J = 1.7 Hz, 1H) 7.72 (d, J = 1.7 Hz, 1H). ^{13}C NMR (50 MHz, $CDCl_3$) δ (ppm): 13.6, 20.0, 25.2, 27.9, 41.5, 44.4, 49.3, 53.8, 54.2, 110.5, 111.6, 125.6, 128.1, 134.0, 135.5, 141.5, 156.5. IR (neat, cm^{-1}): 2931, 1611, 1505, 1465, 1336, 1156, 1037, 815, 729. MS (*m*/*z*): 402 (M + 1). Mp (uncorrected): 186−187 °C. Anal. ($C_{22}H_{30}N_2O_3S$·$C_2H_2O_4$) C, H, N.

4-Methoxy-*N*-[3-(6-methoxy-3,4-dihydro-1*H*-isoquinolin-2-yl)propyl]-benzenesulfonamide (14e). Method A was applied, using **11a** (0.10 g, 0.45 mmol) and *p*-methoxybenzenesulfonyl chloride (0.28 g, 1.36 mmol). This yielded an oil (0.17 g, 97% yield) that was purified by chromatography (Silica, EtOAc/hexane, 2:3) to yield pure **14e** as oil. The free base was converted to its oxalate salt by treatment with oxalic acid dihydrate in ethanol. ^{1}H NMR (free base, 200 MHz, $CDCl_3$) δ (ppm): 1.28 (s, 1H), 1.93−2.12 (m, 5H), 2.52 (t, J = 5.6 Hz, 2H), 2.58 (t, J = 5.6 Hz, 2H), 2.89 (t, J = 5.6 Hz, 2H), 3.53 (s, 1H), 3.79 (s, 3H), 3.89 (s, 3H), 6.67 (m, 5H), 6.98 (d, J = 2.4 Hz, 1H), 7.97 (d, J = 2.2 Hz, 1H). ^{13}C NMR (50 MHz, $CDCl_3$) δ (ppm): 26.1, 28.0, 46.2, 49.3, 53.5, 54.2, 111.3, 111.6, 112.8, 125.5, 126.0, 127.9, 130.3, 134.2, 156.1, 162.2. IR (neat, cm^{-1}): 2926, 1593, 1498, 1366, 1262, 1158, 804. MS (*m*/*z*): 391 (M + 1). Mp (uncorrected): 192−194 °C. Anal. ($C_{20}H_{26}N_2O_4S$·$C_2H_2O_4$) C, H, N.

***N*-Ethyl-4-methoxy-*N*-[3-(6-methoxy-3,4-dihydro-1*H*-isoquinolin-2-yl)propyl]-benzenesulfonamide (14f).** Method A was applied, using **11c** (0.05 g, 0.18 mmol) and *p*-methoxybenzenesulfonyl chloride (0.04 g, 0.21 mmol). This yielded an oil that was purified by chromatography (Silica, CH_2Cl_2/CH_3OH, 99:1) to yield pure **14f** as colorless oil (0.06 g, 80% yield). The free base was converted to its oxalate salt by treatment with oxalic acid dihydrate in ethanol. ^{1}H NMR (free base, 200 MHz, $CDCl_3$) δ (ppm): 1.02 (t, J = 7.2 Hz, 2H), 1.19 (s, 1H), 1.28−1.42 (m, 5H), 3.02−3.22 (m, 6H), 3.49−3.59 (q, J = 7.2 Hz, 3H), 3.73 (s, 3H), 3.81 (s, 3H), 6.63−6.81 (m, 5H), 6.93 (d, J = 8.8 Hz, 1H), 7.68 (d, J = 8.8 Hz, 1H). ^{13}C NMR (50 MHz, $CDCl_3$) δ (ppm): 7.2, 12.2, 22.2, 28.1, 42.0, 44.6, 48.0, 51.5, 53.9, 61.8, 112.5, 112.9, 117.0, 126.0, 126.5, 127.7, 130.4, 158.0, 161.4. IR (neat, cm^{-1}): 2930, 1611, 1498, 1335, 1258, 1152, 1029, 804, 734. MS (*m*/*z*): 419 (M + 1). Mp (uncorrected): 188−190 °C. Anal. ($C_{22}H_{30}N_2O_4S$·$C_2H_2O_4$) C, H, N.

Naphthalene-1-sulfonic Acid [3-(6-Methoxy-3,4-dihydro-1*H*-isoquinolin-2-yl)propyl]amide (14g). Method A was applied, using **11a** (0.09 g, 0.42 mmol) and naphthalene-1-sulfonyl chloride (0.11 g, 0.46 mmol). This yielded a slightly yellow oil (0.17 g) that was purified by chromatography (Silica, CH_2Cl_2/CH_3OH, 99:1) to yield pure **14g** (0.14 g, 81% yield). The free base was converted to its oxalate salt by treatment with oxalic acid dihydrate in ethanol. ^{1}H NMR (free base, 200

MHz, $CDCl_3$) δ (ppm): 0.80−1.00 (m, 2H), 1.28 (s, 1H), 1.71−1.79 (m, 3H), 2.47 (t, J = 5.7 Hz, 2H), 2.70 (t, J = 5.9 Hz, 2H), 2.97 (t, J = 5.3 Hz, 2H), 3.40 (s, 1H), 3.84 (s, 3H), 6.72−6.93 (m, 2H), 7.17−7.28 (m, 2H), 7.51 (t, J = 7.8 Hz, 2H), 7.92 (d, J = 8.3 Hz, 1H), 8.04 (d, J = 1.0 Hz, 1H), 8.24 (d, J = 1.0 Hz, 1H), 8.37 (d, J = 8.8 Hz, 1H). ^{13}C NMR (50 MHz, $CDCl_3$) δ (ppm): 22.9, 27.4, 42.6, 48.1, 54.2, 56.1, 110.8, 111.8, 122.4, 124.8, 125.1, 125.8, 127.2, 128.1, 132.0, 132.5, 134.0, 156.6. IR (neat, cm^{-1}): 2925, 1612, 1505, 1320, 1159, 1135, 773. MS (*m*/*z*): 411 (M + 1). Mp (uncorrected): 170−171 °C. Anal. ($C_{23}H_{26}N_2O_3S\cdot C_2H_2O_4$) C, H, N.

Naphthalene-1-sulfonic Acid Ethyl-[3-(6-methoxy-3,4-dihydro-1*H*-isoquinolin-2-yl)propyl]amide (14h). Method A was applied, using **11c** (0.09 g, 0.36 mmol) and naphthalene-1-sulfonyl chloride (0.09 g, 0.39 mmol). This yielded an oil (0.11 g, 70% yield) that was purified by chromatography (Silica, CH_2Cl_2/CH_3OH, 99:1) to yield pure **14h** as oil. The free base was converted to its oxalate salt by treatment with oxalic acid dihydrate in ethanol. ^{1}H NMR (free base, 200 MHz, $CDCl_3$) δ (ppm): 1.11 (t, J = 7.2 Hz, 2H), 1.26 (s, 1H), 1.74−1.81 (m, 5H), 2.33 (t, J = 7.1 Hz, 2H), 2.54 (t, J = 19.2 Hz, 2H), 2.79 (t, J = 4.9 Hz, 2H), 3.33−3.49 (m, 3H), 3.78 (d, J = 7.6 Hz, 1H), 6.62−6.72 (m, 2H), 6.89 (d, J = 8.6 Hz, 1H), 7.47−7.65 (m, 3H), 7.93 (d, J = 7.6 Hz, 1H), 8.03 (d, J = 8.5 Hz, 1H), 8.23 (d, J = 1.2 Hz, 1H), 8.65 (d, J = 9.3 Hz, 1H). ^{13}C NMR (50 MHz, $CDCl_3$) δ (ppm): 12.1, 24.3, 27.8, 40.0, 43.0, 49.1, 53.6, 53.7, 53.9, 110.5, 111.6, 122.6, 123.6, 125.3, 126.0, 126.5, 127.4, 128.2, 132.5, 133.8. IR (neat, cm^{-1}): 2925, 1612, 1505, 1320, 1259, 1135, 773. MS (*m*/*z*): 439 (M + 1). Mp (uncorrected): 166−169 °C. Anal. ($C_{25}H_{30}N_2O_3S\cdot C_2H_2O_4$) C, H, N.

(5-Methoxy-1*H*-indol-3-yl)oxoacetyl Chloride (16). Oxalyl chloride (1.00 g, 8.16 mmol) was dissolved in dry diethyl ether (15 mL) and cooled to 0 °C. 5-Methoxyindole (**15**, 1.00 g, 6.80 mmol) was added portionwise. The bright orange precipitate thus formed was filtered after 30 min, dried in vacuo (1.45 g, 75% yield), and used without further purification. IR (KBr, cm^{-1}): 3193, 1779, 1617, 1477, 1427, 1267, 1211, 991, 773, 705, 653.

2-(5-Methoxy-1*H*-indol-3-yl)-*N*,*N*-dimethyl-2-oxoacetamide (17). (5-Methoxy-1*H*-indol-3-yl)oxoacetyl chloride (**16**, 0.25 g, 1.05 mmol) was added portionwise to a solution of dimethylamine (5 mL, 40% in water) at 0 °C. After 30 min, CH_2Cl_2 (50 mL) was added. The layers were separated, and the inorganic phase was washed with CH_2Cl_2. The combined organic layers were dried (Na_2SO_4), filtered, and concentrated in vacuo. The residue was crystallized from EtOAc/hexanes to yield a white solid (0.23 g, 89% yield). ^{1}H NMR (200 MHz, CD_3OD/$CDCl_3$) δ (ppm): 2.80 (d, J = 8.8 Hz, 6H), 3.64 (d, 8.8 Hz, 3H), 6.66 (s, 1H), 7.08 (d, J = 8.1 Hz), 7.50 (s, 1H), 7.58 (s, 1H). IR (KBr, cm^{-1}): 3090, 3038, 2894, 1605, 1518, 1490, 1437, 1265, 1210, 1149, 1030, 808.

[2-(5-Methoxy-1*H*-indol-3-yl)ethyl]-dimethylamine (18). In a three-necked bottle with cooler, $LiAlH_4$ (0.11 g, 2.89 mmol) was suspended in THF (10 mL) under nitrogen atmosphere. 2-(5-methoxy-1*H*-indol-3-yl)-*N*,*N*-dimethyl-2-oxoacetamide (**17**, 0.20 g, 0.81 mmol), dissolved in THF (10 mL) was added dropwise at room temperature. The suspension was heated to a gentle reflux for 2 h. After cooling to room temperature, the excess of $LiAlH_4$ was destroyed by careful addition of adequate amounts of water and NaOH (4 N). The salts were filtered over Celite and washed well (diethyl ether), and the residue was concentrated in vacuo to yield a colorless oil (0.14 g, 79% yield), which was pure **18** according to NMR and GC. ^{1}H NMR (200 MHz, $CDCl_3$) δ (ppm): 2.31 (s, 6H), 2.61 (dd, J_a = 7.3 Hz, J_b = 8.8 Hz, 2H), 2.87 (dd, J_a = 7.3 Hz, J_b = 8.8 Hz, 2H), 3.81 (s, 3H), 6.80 (dd, J_a = 2.6 Hz, J_b = 6.2 Hz, 1H), 6.91, (s, 1H), 6.99 (d, J = 2.2 Hz, 1H), 7.15 (d, J = 8.8 Hz, 1H). ^{13}C NMR (75 MHz, $CDCl_3$) δ (ppm): 21.2, 42.9, 53.5, 57.7, 98.2, 109.4, 109.5, 111.3, 120.0, 125.3, 129.0, 151.3. IR (free base, neat, cm^{-1}): 3410, 3145, 2930, 2800, 1623, 1580, 1485, 1215, 1171, 1066, 795. MS (EI$^+$): 218, 160, 117, 89, 58 (100%).

[2-(5-Methoxy-1-methyl-1*H*-indol-3-yl)ethyl]dimethylamine (19). In a three-necked bottle with cooler, [2-(5-methoxy-1*H*-indol-3-yl)ethyl]dimethylamine (**18**, 0.18 g, 0.83 mmol) was dissolved in DMF under nitrogen atmosphere. After addition of KO-*t*-Bu (0.10 g, 0.89 mmol) and dimethyl oxalate (0.10 g, 0.85 mmol), the mixture was heated to reflux for 4 h. The mixture was then allowed to cool to room temperature, and ammonia (30 mL, 10% in water) was added. Extraction with diethyl ether (3 × 15 mL), drying (Na_2SO_4) of the combined organic layers, and subsequent evaporation of the volatiles yielded a brown oil (0.17 g, 86% yield), which was purified by chromatography (Silica, gradient CH_2Cl_2/CH_3OH: 100/0−85/15). The free base was converted to its oxalate salt by treatment with oxalic acid dihydrate in ethanol. ^{1}H NMR (300 MHz, $CDCl_3$) δ (ppm): 2.30 (s, 6H), 2.57 (dd, J_a = 7.3 Hz, J_b = 8.4 Hz, 2H), 2.82−2.89 (m, 2H), 3.63 (s, 3H), 3.82 (s, 3H), 6.80 (s, 1H), 6.84 (dd, J_a = 2.2 Hz, J_b = 6.6 Hz, 1H), 7.00 (d, J = 1.8 Hz, 1H), 7.12 (d, J = 8.8 Hz, 1H). ^{13}C NMR (75 MHz, $CDCl_3$) δ (ppm): 21.2, 30.2, 43.0, 53.5, 58.0, 98.4, 107.5, 109.1, 109.7, 124.5, 125.6, 129.9, 151.1. MS (EI$^+$): 232, 174, 131, 58 (100%). Anal. ($C_{14}H_{20}N_2O\cdot C_2H_2O_4$) C, H, N.

3-(1-Benzyl-1,2,3,6-tetrahydropyridin-4-yl)-5-methoxy-1*H*-indole (20). In a three-necked bottle with cooler, 5-methoxyindole (**15**, 0.50 g, 3.40 mmol) was dissolved in CH_3OH (5 mL) under nitrogen atmosphere. *N*-Benzyl-4-piperidone (0.96 g, 5.08 mmol) and $NaOCH_3$ (5 mL, 30% solution in CH_3OH) were added, and the mixture was heated to reflux for 4 h. The reaction was allowed to cool to room temperature. The precipitate that was formed, filtered off (0.90 g, 83% yield), and dried in vacuo. Recrystallization from EtOAc yielded pure **20** as a white solid. ^{1}H NMR (300 MHz, $CDCl_3$) δ (ppm): 2.53 (d, J = 1.5 Hz, 2H), 2.68−2.72 (m, 2H), 3.20 (dd, J_a = 2.6 Hz, J_b = 2.9 Hz, 2H), 3.62 (s, 2H), 3.80 (s, 3H), 6.07−6.09 (m, 1H), 6.79−6.83 (m, 1H), 7.07 (d, J = 2.6 Hz, 1H), 7.17−7.38 (m, 7H), 8.00 (br, 1H). ^{13}C NMR (75 MHz, $CDCl_3$) δ (ppm): 26.7, 47.6, 50.8, 53.5, 60.5, 100.5, 109.3, 109.7, 116.4, 119.5, 123.1, 124.6, 125.8, 126.8, 127.4, 151.9. IR (KBr, cm^{-1}): 3032, 2925, 2854, 2794, 1650, 1614, 1601, 1479, 1447, 1380, 1260, 1211, 1125, 1034, 962, 880, 807, 736. MS (EI$^+$): 318, 227, 198, 160, 128, 91 (100%). Anal. ($C_{21}H_{22}N_2O$) C, H, N.

6-Methoxy-2,3-dihydro-1*H*-indole (22). 6-Methoxy-1*H*-indole (**21**, 1.50 g, 10.2 mmol) was dissolved in glacial acetic acid (30 mL). $NaCNBH_3$ (1.9 g, 30.6 mmol) was added portionwise, while the temperature did not exceed 20 °C. After stirring at room temperature for 3 h, the solvent was removed under reduced pressure, and the residue was treated with $NaHCO_3$ (150 mL, sat.). The water layer was extracted with ether (3 × 75 mL), and the combined organic phase was washed with brine (30 mL), dried (Na_2SO_4), and filtered. Evaporation of solvent yielded a colorless oil (1.48 g, 97% yield), that could be purified by chromatography (Silica, CH_2Cl_2) to obtain pure **22**. ^{1}H NMR (200 MHz, $CDCl_3$) δ (ppm): 2.95 (t, J = 16.6 Hz, 2H), 3.55 (t, J = 16.6 Hz, 2H), 3.75 (s, 3H), 3.88 (br, 1H), 6.26 (s, 1H), 6.30 (d, J = 2.4 Hz, 1H), 7.00 (d, J = 10.7 Hz, 1H). ^{13}C NMR (50 MHz, $CDCl_3$) δ (ppm): 27.5, 53.9, 95.1, 102.2, 120.2, 123.3, 151.1, 158.3. IR (neat, cm^{-1}): 3375, 2947, 2847, 1614, 1500, 1286, 1196, 1150, 1030, 830. MS (EI$^+$): 149 (100%), 133, 117, 104, 91, 77, 63, 51.

2-Chloro-1-(6-methoxy-2,3-dihydroindol-1-yl)ethanone (23). A solution of 6-Methoxy-2,3-dihydro-1*H*-indole (**22**, 2.20 g, 14.8 mmol) in CH_2Cl_2 (35 mL) was added dropwise to a mixture of chloroacetyl chloride (3.35 g, 29.5 mmol) and K_2CO_3 (4.50 g, 32.6 mmol) in CH_2Cl_2 (75 mL). After addition, the suspension was stirred at room temperature for 6 h. Water (100 mL) was added and extracted with CH_2Cl_2 (3 × 50 mL). The combined organic layers were washed with brine (20 mL), dried (Na_2SO_4), and filtered. Evaporation of the solvent yielded an off-white solid (2.95 g, 88% yield). Pure **23** was obtained by recrystallization from diisopropyl ether. ^{1}H NMR (200 MHz, $CDCl_3$) δ (ppm): 3.17 (t, J = 16.4 Hz, 2H), 3.80 (s, 3H), 4.16 (s, 2H), 4.17 (t, J = 16.6 Hz, 2H), 6.62 (d, J = 10.5 Hz, 1H), 7.07 (d, J = 8.1 Hz, 1H), 7.90 (s, 1H). ^{13}C NMR (50 MHz, $CDCl_3$) δ (ppm): 25.9, 41.7, 47.2, 54.1, 101.6, 109.5, 123.2. IR (KBr, cm^{-1}): 2964, 1680, 1497, 1404, 1231, 1028, 842. Mp (uncorrected): 126 °C

2-Dimethylamino-1-(6-methoxy-2,3-dihydroindol-1-yl)-ethanone (24). Dimethylamine hydrochloride (0.18 g, 2.20

mmol) was added to a suspension of 2-chloro-1-(6-methoxy-2,3-dihydroindol-1-yl)ethanone (**23**, 0.50 g, 2.20 mmol) and K_2CO_3 (0.61 g, 4.42 mmol) in acetonitrile (25 mL, cat. amount DMF) under a nitrogen atmosphere. The mixture was stirred overnight at 50 °C. After filtration, the volatiles were removed in vacuo to yield the crude **24** as a semisolid (0.51 g, 99% yield), which was used for reduction without further purification. ^{1}H NMR (200 MHz, $CDCl_3$) δ (ppm): 2.35 (s, 3H), 3.05 (t, J = 16.6 Hz, 2H), 3.16 (s, 2H), 3.76 (s, 3H), 4.11 (t, J = 16.8 Hz, 2H), 6.53 (d, J = 10.5 Hz, 1H), 7.00 (d, J = 8.1 Hz, 1H), 7.89 (s, 1H). ^{13}C NMR (50 MHz, $CDCl_3$) δ (ppm): 25.9, 44.1, 46.7, 54.0, 62.0, 101.4, 108.5, 123.1. IR (KBr, cm^{-1}): 2933, 2827, 2772, 1654, 1492, 1283, 1157, 1029, 859. MS (EI$^+$): 234, 58 (100%).

[2-(6-Methoxy-2,3-dihydroindol-1-yl)ethyl]dimethylamine (25). $LiAlH_4$ (0.26 g, 6.84 mmol) was suspended in THF (25 mL) under nitrogen atmosphere and cooled to 0 °C. $AlCl_3$ (1.07 g, 8.04 mmol) was carefully added and stirred for 15 min. Then, a solution of 2-(dimethylamino)-1-(6-methoxy-2,3-dihydroindol-1-yl)ethanone (**24**, 0.51 g, 2.20 mmol) in THF (10 mL) was added dropwise. The reaction was stirred at room temperature for 4 h. Careful workup of the reaction by addition of water and NaOH (1 N) resulted in formation of salts, which were filtered off over Celite. The mother liquor was concentrated in vacuo, and the remainder was partioned between $NaHCO_3$ (30 mL, sat.) and CH_2Cl_2 (50 mL). The organic phase was dried (Na_2SO_4), filtered, and concentrated in vacuo. Purification by chromatography (Silica, gradient CH_2Cl_2/CH_3-OH: 100/0−85/15) yielded pure **25** as a colorless oil (0.21 g, 43% yield). The free base was converted to its oxalate salt by treatment with oxalic acid dihydrate in ethanol. ^{1}H NMR (free base, 200 MHz, $CDCl_3$) δ (ppm): 2.26 (s, 6H), 2.49 (t, J = 14.3 Hz, 2H), 2.84 (t, J = 16.5 Hz, 2H), 3.13 (t, J = 14.3 Hz, 2H), 3.35 (t, J = 16.5 Hz, 2H), 3.71 (s, 3H), 6.03 (s, 1H), 6.11 (d, J = 10.3 Hz, 1H), 6.88 (d, J = 8.1 Hz, 1H). ^{13}C NMR (50 MHz, $CDCl_3$) δ (ppm): 25.3, 43.3, 45.1, 51.6, 52.9, 54.3, 92.0, 98.7, 119.8, 121.8, 151.3, 157.6. IR (neat, cm^{-1}): 2942, 2819, 2767, 1616, 1495, 1281, 1205, 1034, 818. MS (EI$^+$): 220, 162, 58 (100%). Anal. ($C_{13}H_{20}N_2O\cdot C_2H_2O_4$) C, H, N.

2-Amino-4-methoxyphenol (27). 4-Methoxy-2-nitrophenol (**26**, 1.00 g, 5.9 mmol) was dissolved in ethanol (100 mL, absol) with palladium (0.15 g, 10% on charcoal) and allowed to react for 20 min at room temperature with hydrogen gas (35 psi) in a Parr-shaker. The reaction mixture was filtered over Celite, and the solvent was removed under reduced pressure. This yielded pure **27** as an off-white solid (0.80 g, 98% yield). ^{1}H NMR (300 MHz, $CDCl_3$) δ (ppm): 2.57 (br, 3H), 3.63 (s, 3H), 6.10 (dd, J_a = 2.6 Hz, J_b = 2.9 Hz, 1H), 6.25 (d, J = 2.6 Hz, 1H), 6.55 (d, J = 8.4 Hz, 1H). ^{13}C NMR (75 MHz, $CDCl_3$) δ (ppm): 53.1, 100.3, 100.8, 113.1, 133.2, 135.9, 151.4. IR (KBr, cm-^{1}): 3383, 3292, 2960, 2832, 2591, 1600, 1514, 1465, 1310, 1234, 1201, 1032, 839, 802. MS (EI$^+$): 139, 96 (100), 68.

6-Methoxy-4*H*-benzo[1,4]oxazin-3-one (28). ***27*** (0.25 g, 1.8 mmol) was dissolved in acetonitrile (15 mL) in a three-necked bottle with reflux condenser under nitrogen. 2-Chloroacetyl chloride (0.22 g, 2.0 mmol) was added dropwise, followed by K_2CO_3 (0.65, 4.7 mmol). The suspension was refluxed for 2 h, then cooled to room temperature and filtered. The solution was concentrated in vacuo, and the residue was partioned between CH_2Cl_2 (3 × 15 mL) and water (30 mL). The combined organic layers were dried (Na_2SO_4), filtered, and concentrated to yield **28** as a slightly pink solid (0.31 g, 87% yield) that was recrystallized from methanol. ^{1}H NMR (300 MHz, $CDCl_3$) δ (ppm): 3.71 (s, 3H), 4.51 (s, 2H), 6.34 (d, J = 2.9 Hz, 1H), 6.46 (dd, J_a = 2.6 Hz, J_b = 6.2 Hz, 1H) 6.84 (d, J = 8.8 Hz, 1H), 8.59 (br, 1H). ^{13}C NMR (50 MHz, $CDCl_3$) δ (ppm): 53.3, 64.9, 99.6, 106.3, 114.7. IR (KBr, cm-^{1}): 3197, 3106, 2898, 1712, 1610, 1518, 1464, 1398, 1215, 1048, 830. MS (EI$^+$): 179 (100), 109

6-Methoxy-3,4-dihydro-2*H*-benzo[1,4]oxazine (29). In a round-bottom flask $LiAlH_4$ (0.10 g, 2.1 mmol) was suspended in THF (25 mL, dry) under nitrogen atmosphere. **28** (0.18 g, 1.0 mmol) was added portionwise, and the reaction was allowed to stir overnight at room temperature. The excess of $LiAlH_4$ was decomposed by careful subsequent addition of water (5 drops), NaOH (2 N, 5 drops), and water (ca 0.2 mL). The salts thus formed were filtered over $MgSO_4$, and the solvent was evaporated to yield **29** (0.15 g, 91% yield) as slightly green oil that crystallized upon standing and needed no further purification. ^{1}H NMR (300 MHz, $CDCl_3$) δ (ppm): 3.32−3.35 (m, 2H), 3.66 (s, 3H), 3.73 (br, 1H), 4.14 (t, J = 4.4 Hz, 2H), 6.12 (d, J = 2.6 Hz, 1H), 6.17 (dd, J_a = 2.6 Hz, J_b = 2.9 Hz, 1H), 6.65 (d, J = 8.8 Hz, 1H). ^{13}C NMR (75 MHz, $CDCl_3$) δ (ppm): 38.6, 53.1, 62.5, 98.8, 101.0, 114.4, 131.6, 135.7, 151.9. IR (KBr, cm^{-1}): 3389, 2947, 1620, 1514, 1204, 1167, 1047, 835, 782. MS (EI$^+$): 165 (100), 150, 79, 68, 55.

[2-(6-Methoxy-2,3-dihydrobenzo[1,4]oxazin-4-yl)ethyl]-dimethylamine Hydrochloride (32). 6-Methoxy-3,4-dihydro-2*H*-benzo[1,4]oxazine (**29**, 0.17 g, 1.03 mmol), 2-chloroacetyl chloride (0.12 g, 1.07 mmol), and pyridine (0.15 mL) were stirred at room temperature overnight under nitrogen. The volatiles were evaporated, and the residue was partioned between water and CH_2Cl_2. The organic layer was dried (Na_2SO_4), filtered, and concentrated in vacuo to yield **30** as a brown oil (0.25 g, 100% yield). (MS (EI$^+$): 241 (100%), 165, 150, 137, 109, 77). The brown oil obtained was dissolved in acetonitrile (10 mL) under nitrogen. K_2CO_3 (0.28 g, 2.03 mmol), KI (1 small crystal), and dimethylamine hydrogen chloride (0.15 g, 1.83 mmol) were added. The mixture was stirred at room temperature for 20 h. The volatiles were removed under reduced pressure, and the residue was partioned between acid (HCl, 1 M) and ether. The water layer was made alkaline (NaOH, 2 N, pH = 8) and subsequently extracted with CH_2Cl_2. The organic layer was dried (Na_2SO_4), filtered, and concentrated in vacuo to yield crude **31** as a brown oil (0.13 g, 52% yield, MS (EI$^+$): 250, 58 (100%), IR (KBr): 2943, 2827, 2776, 1660, 1502, 1397, 1254, 1212, 1175, 1058, 860). This oil, dissolved in THF (5 mL), was added dropwise to a suspension of $AlCl_3$ (0.13 g, 0.98 mmol) and $LiAlH_4$ (0.04 g, 1.05 mmol) in diethyl ether. The reaction was allowed to stir at room temperature for 4 h and was then carefully quenched with water and neutralized with $NaHCO_3$ (saturated aqueous solution). Extraction with diethyl ether and subsequent drying (Na_2SO_4), filtration, and evaporation of the organic layer yielded a brown oil (0.11 g, 47% yield) that was purified by chromatography to yield pure **32** as a colorless oil (Silica, CH_2Cl_2/CH_3OH 98:2). The compound was converted in its hydrochloride by treatment of the free base in 2-propanol with HCl (1 N solution in diethyl ether, 1 equiv). ^{1}H NMR (free base, 300 MHz, $CDCl_3$) δ (ppm): 2.23 (s, 6H), 2.42−2.47 (m, 2H), 3.28−3.33 (m, 4H), 3.68 (s, 3H), 4.10 (t, J = 4.4 Hz, 2H), 6.06−6.09 (m, 1H), 6.20 (d, J = 2.6 Hz, 1H), 6.62 (d, J = 8.8 Hz, 1H). ^{13}C NMR (75 MHz, $CDCl_3$) δ (ppm): 43.4, 45.0, 46.8, 53.0, 53.1, 61.8, 96.2, 98.1, 113.7, 133.1, 135.7, 152.3. IR (neat, cm^{-1}): 2940, 2821, 2768, 1618, 1511, 1463, 1314, 1207, 1171, 1050, 823. MS (EI$^+$): 236, 178, 150, 58 (100%). Anal. ($C_{13}H_{20}N_2O_2\cdot$HCl_H_2O) C, H, N, O.

Pharmacology. 5-HT$_7$ Receptor Binding Assay. Binding assays on membranes from HEK cells expressing rat 5-HT$_7$ (r5-HT$_7$ receptor obtained from Dr. David Sibley) receptors were performed according to standard procedures. Briefly, cell paste was homogenized in 50 mM Tris HCl buffer (pH 7.4) containing 2.0 mM $MgCl_2$ using a hand-held Polytron (setting 6 for 10 s) and spun in a centrifuge at 40 000 g for 10 min. The pellet was resuspended in 50 mM Tris HCl buffer (pH 7.4) containing 0.5 mM EDTA, 10 mM $MgSO_4$, 2 mM $CaCl_2$, 10 μM pargyline, and 0.1% ascorbic acid. Incubations were initiated by the addition of membranes (20 μg protein per well) to 96-well plates containing test drugs and 0.3 nM [^{3}H]5-CT (final volume of 250 μL). Nonspecific binding was determined by radioligand binding in the presence of a saturating concentration of 5-HT (10 μM). After a 2-h incubation period at room temperature, assay samples were rapidly filtered through Whatman GF/B filters and rinsed with ice-cold 50 mM Tris buffer (pH 7.4) using a Skatron harvester (Molecular Devices). Membrane-bound [^{3}H]5-CT levels were determined by liquid scintillation counting of the filters in BetaScint. The IC_{50} value (concentration at which 50% inhibition of specific binding

occurs) was calculated by linear regression of the log concentration−response data. K_i values were calculated according to the Cheng−Prusoff equation, $K_i = IC_{50}/(1 + (L/K_d))$, where L is the concentration of the radioligand used in the experiment and the K_d value is the dissociation constant for the radioligand (determined previously by saturation analysis).

5-HT$_7$ Adenylate Cyclase Assay. Effects on adenylate cyclase activity were measured according to previously published methods.[37] HEK-293 cells expressing the rat 5-HT$_7$ were grown in Dulbecco's modified Eagle's media (DMEM) containing 10% fetal bovine serum, 400 μg of G418 (Geneticin), and 2 mM glutamine until flasks were confluent. Cells from confluent flasks were harvested by replacing the media with phosphate-buffered saline (PBS) containing 5 mM EDTA (pH 7.4). Cells were homogenized in 5 mM HEPES buffer containing 1 mM EGTA (pH 7.4) using a hand-held glass−Teflon homogenizer. The homogenate was centrifuged in 35 000 g for 10 min. The cell pellet was resuspended in 100 mM HEPES buffer containing 1 mM EGTA (pH 7.4). Membranes (30−40 μg protein) were incubated at 37°C in a reaction medium containing 100 mM HEPES (pH 7.4), 5.0 mM $MgCl_2$, 0.5 mM ATP, 1.0 mM cAMP, 0.5 mM IBMX, 10 mM phosphocreatine, 0.31 mg/mL creatine phosphokinase, 100 μM GTP, 1 μCi α-[^{33}P]ATP per tube, and test drugs (final volume of 100 μL)**.** Incubations were terminated after 15 min by adding 2% sodium dodecyl sulfate. After separation of [^{33}P]cAMP from [^{33}P]ATP as described by Salomon,[37] [^{33}P]cAMP levels were determined by liquid scintillation counting, with the results expressed as picomoles per minute per milligram of protein. EC_{50} and IC_{50} values were calculated by linear regression analysis of the concentration−response curves. Efficacy values were calculated as the maximal effect of an agonist in terms of the maximal effect produced by a known agonist such as 5-HT. Apparent K_i values for antagonists were calculated as follows: $K_i = IC_{50}/(1 + (C/EC_{50}))$, where C is the concentration of the agonist used in the experiment and EC_{50} is the EC_{50} for the agonist.

Supporting Information Available: Table of elemental analyses. This material is available free of charge via the Internet at http://pubs.acs.org.

References

(1) Pallas. [Version 1.2]. 1994. CompuDrug Chemistry Ltd.
(2) MacroModel. [Version 7.0]. 1999. Schrodinger Inc.
(3) Sybyl Molecular Modeling Software. [Version 6.8]. 2001. Tripos, Inc.
(4) Allinger, N. L.; Yuh, Y. H.; Lii, J.-H. Molecular mechanics. The MM3 force field for hydrocarbons. 1. *J. Am. Chem. Soc.* **1989**, *111*, 8551−8566.
(5) Baldwin, J. M.; Schertler, G. F. X.; Unger, V. M. An alpha-carbon template for the transmembrane helices in the rhodopsin family of G-protein-coupled receptors. *J. Mol. Biol.* **1997**, *272*, 144−164.
(6) Ballesteros, J. A.; Weinstein, H. Integrated methods for the construction of three-dimensional models and computational probing of structure−function relations in G protein-coupled receptors. *Methods Neurosci.* **1995**, *25*, 366−428.
(7) Bard, J. A.; Zgombick, J.; Adham, N.; Vaysse, P.; Branchek, T. A.; Weinshank, R. L. Cloning of a novel human serotonin receptor (5-HT7) positively linked to adenylate cyclase. *J. Biol Chem.* **1993**, *268*, 23422−23426.
(8) Bojarski, A. J.; Mokrosz, M. J. 1,2,3,4-Tetrahydroisoquinoline derivatives; lipophilicity evaluation vs 5-HT1A receptor affinity. *Pharmazie* **1999**, *54*, 828−830.
(9) Bojarski, A. J.; Mokrosz, M. J.; Minol, S. C.; Koziol, A.; Wesolowska, A.; Tatarczynska, E.; Klodzinska, A.; Chojnacka-Wojcik, E. The influence of substitution at aromatic part of 1,2,3,4-tetrahydroisoquinoline on in vitro and in vivo 5-HT(1A)/5-HT-(2A) receptor activities of its 1-adamantoyloaminoalkyl derivatives. *Bioorg. Med. Chem.* **2002**, *10*, 87−95.
(10) Chang, G.; Guida, W. C.; Still, W. C. An internal-coordinate Monte Carlo method for searching conformational space. *J. Am. Chem. Soc.* **1989**, *111*, 4379−4386.
(11) Decker, H.; Becker, P. *Liebigs Ann. Chem.* **1913**, *395*, 342.
(12) Forbes, I. T.; Dabbs, S.; Duckworth, D. M.; Jennings, A. J.; King, F. D.; Lovell, P. J.; Brown, A. M.; Collin, L.; Hagan, J. J.; Middlemiss, D. N.; Riley, G. J.; Thomas, D. R.; Upton, N. (*R*)-3,*N*-dimethyl-*N*-[1-methyl-3-(4-methyl-piperidin-1-yl)propyl]benzenesulfonamide: The first selective 5-HT7 receptor antagonist. *J. Med. Chem.* **1998**, *41*, 655−657.
(13) Forbes, I. T.; Douglas, S.; Gribble, A. D.; Ife, R. J.; Lightfoot, A. P.; Garner, A. E.; Riley, G. J.; Jeffrey, P.; Stevens, A. J.; Stean, T. O.; Thomas, D. R. SB-656104-A: a novel 5-HT(7) receptor antagonist with improved in vivo properties. *Bioorg. Med. Chem. Lett.* **2002**, *12*, 3341−3344.
(14) Goodman, J.; Still, W. C. An unbounded systematic search of conformational space. *J. Comput. Chem.* **1991**, *12*, 1110−1117.
(15) Hagan, J. J.; Price, G. W.; Jeffrey, P.; Deeks, N. J.; Stean, T.; Piper, D.; Smith, M. I.; Upton, N.; Medhurst, A. D.; Middlemiss, D. N.; Riley, G. J.; Lovell, P. J.; Bromidge, S. M.; Thomas, D. R. Characterization of SB-269970-A, a selective 5-HT7 receptor antagonist. *Br. J. Pharmacol.* **2000**, *130*, 539−548.
(16) Javitch, J. A.; Ballesteros, J. A.; Weinstein, H.; Chen, J. A cluster of aromatic residues in the sixth membrane-spanning segment of the dopamine D2 receptor is accessible in the binding-site crevice. *Biochemistry* **1998**, *37*, 998−1006.
(17) Kikuchi, C.; Ando, T.; Watanabe, T.; Nagaso, H.; Okuno, M.; Hiranuma, T.; Koyama, M. 2a-[4-(Tetrahydropyridoindol-2-yl)-butyl]tetrahydrobenzindole derivatives: new selective antagonists of the 5-hydroxytryptamine7 receptor. *J. Med. Chem* **2002**, *45*, 2197−2206.
(18) Kikuchi, C.; Hiranuma, T.; Koyama, M. Tetrahydrothienopyridylbutyl-tetrahydrobenzindoles: new selective ligands of the 5-HT(7) receptor. *Bioorg. Med. Chem. Lett.* **2002**, *12*, 2549−2552.
(19) Kikuchi, C.; Nagaso, H.; Hiranuma, T.; Koyama, M. Tetrahydrobenzindoles: Selective antagonists of the 5-HT7 receptor. *J. Med. Chem.* **1999**, *42*, 533−535.
(20) Kikuchi, C.; Suzuki, H.; Hiranuma, T.; Koyama, M. New tetrahydrobenzindoles as potent and selective 5-HT7 antagonists with increased In vitro metabolic stability. *Bioorg. Med. Chem. Lett.* **2003**, *13*, 61−64.
(21) Krobert, K. A.; Bach, T.; Syversveen, T.; Kvingedal, A. M.; Levy, F. O. The cloned human 5-HT7 receptor splice variants: A comparative characterization of their pharmacology, function and distribution. *Naunyn S. Arch. Pharmacol.* **2001**, *363*, 620−632.
(22) Krobert, K. A.; Levy, F. O. The human 5-HT7 serotonin receptor splice variants: constitutive activity and inverse agonist effects. *Br. J. Pharmacol.* **2002**, *135*, 1563−1571.
(23) Lii, J.-H.; Allinger, N. L. Molecular mechanics. The MM3 force field for hydrocarbons. 2. Vibrational frequencies and thermodynamics. *J. Am. Chem. Soc.* **1989**, *111*, 8566−8575.
(24) Lii, J.-H.; Allinger, N. L. Molecular mechanics. The MM3 force field for hydrocarbons. 3. The van der Waals' potentials and crystal data for aliphatic and aromatic hydrocarbons. *J. Am. Chem. Soc.* **1989**, *111*, 8576−8582.
(25) Linnanen, T.; Brisander, M.; Unelius, L.; Rosqvist, S.; Nordvall, G.; Hacksell, U.; Johansson, A. M. Atropisomeric derivatives of 2′,6′-disubstituted (R)-11- phenylaporphine: selective serotonin 5-HT(7) receptor antagonists. *J. Med. Chem.* **2001**, *44*, 1337−1340.
(26) Lopez-Rodriguez, M. L.; Porras, E.; Benhamu, B.; Ramos, J. A.; Morcillo, M. J.; Lavandera, J. L. First pharmacophoric hypothesis for 5-HT7 antagonism. *Bioorg. Med. Chem. Lett.* **2000**, *10*, 1097−1100.
(27) Lopez-Rodriguez, M. L.; Porras, E.; Morcillo, M. J.; Benhamu, B.; Soto, L. J.; Lavandera, J. L.; Ramos, J. A.; Olivella, M.; Campillo, M.; Pardo, L. Optimization of the pharmacophore model for 5-HT7R antagonism. Design and synthesis of new naphtholactam and naphthosultam derivatives. *J. Med. Chem.* **2003**, *46*, 5638−5650.
(28) Lovell, P. J.; Bromidge, S. M.; Dabbs, S.; Duckworth, D. M.; Forbes, I. T.; Jennings, A. J.; King, F. D.; Middlemiss, D. N.; Rahman, S. K.; Saunders: D. V.; Collin, L. L.; Hagan, J. J.; Riley, G. J.; Thomas, D. R. A novel, potent, and selective 5-HT7 antagonist: (*R*)-3-(2-(2-(4-methylpiperidin-1-yl)-ethyl)pyrrolidine-1-sulfonyl)phenol (SB-269970). *J. Med. Chem.* **2000**, *43*, 342−345.
(29) Lovenberg, T. W.; Baron, B. M.; de Lecea, L.; Miller, J. D.; Prosser, R. A.; Rea, M. A.; Foye, P. E.; Racke, M.; Slone, A. L.; Siegel, B. W. A novel adenylyl cyclase-activating serotonin receptor (5-HT7) implicated in the regulation of mammalian circadian rhythms. *Neuron* **1993**, *11*, 449−458.
(30) Mokrosz, J. L.; Bojarski, A. J.; Charakchieva-Minol, S.; Duszynska, B.; Mokrosz, M. J.; Paluchowska, M. H. Structure−activity relationship studies of CNS agents, Part 23: N-(3-phenylpropyl)- and N-[(E)-cinnamyl]-1,2,3,4-tetrahydroisoquinoline mimic 1-phenylpiperazine at 5-HT1A receptors. *Arch. Pharm. (Weinheim)* **1995**, *328*, 604−608.
(31) Mokrosz, J. L.; Deren-Wesolek, A.; Tatarczynska, E.; Duszynska, B.; Bojarski, A. J.; Mokrosz, M. J.; Chojnacka-Wojcik, E. 8-[4-[2-(1,2,3,4-Tetrahydroisoquinolinyl]butyl-8-azaspiro[4.5]-decane -7,9-dione: a new 5-HT1A receptor ligand with the same activity profile as buspirone. *J. Med. Chem.* **1996**, *39*, 1125−1129.

(32) Mokrosz, M. J.; Bojarski, A. J.; Duszynska, B.; Tatarczynska, E.; Klodzinska, A.; Deren-Wesolek, A.; Charakchieva-Minol, S.; Chojnacka-Wojcik, E. 1,2,3,4-tetrahydroisoquinoline derivatives: a new class of 5-HT1A receptor ligands. *Bioorg. Med. Chem* **1999**, *7*, 287−295.
(33) Paluchowska, M. H.; Bojarski, A. J.; Charakchieva-Minol, S.; Wesolowska, A. Active conformation of some arylpiperazine postsynaptic 5-HT(1A) receptor antagonists. *Eur. J. Med. Chem.* **2002**, *37*, 273−283.
(34) Perrone, R.; Berardi, F.; Colabufo, N. A.; Lacivita, E.; Leopoldo, M.; Tortorella, V. Synthesis and structure-affinity relationships of 1-[*o*mega-(4-aryl-1-piperazinyl)alkyl]-1-aryl ketones as 5-HT-(7) receptor ligands. *J. Med. Chem.* **2003**, *46*, 646−649.
(35) Plassat, J. L.; Amlaiky, N.; Hen, R. Molecular cloning of a mammalian serotonin receptor that activates adenylate cyclase. *Mol. Pharmacol.* **1993**, *44*, 229−236.
(36) Ruat, M.; Traiffort, E.; Leurs, R.; Tardivel Lacombe, J.; Diaz, J.; Arrang, J.; Schwartz, J. C. Molecular cloning, characterization, and localization of a high-affinity serotonin receptor (5-HT7) activating cAMP formation. *Proc. Natl. Acad. Sci U.S.A.* **1993**, *90*, 8547−8551.
(37) Salomon, Y. Adenylate cyclase assay. *Adv. Cyclic Nucleotide Res.* **1979**, *10*, 35−55.
(38) Shapiro, D. A.; Kristiansen, K.; Kroeze, W. K.; Roth, B. L. Differential modes of agonist binding to 5-hydroxytryptamine-(2A) serotonin receptors revealed by mutation and molecular modeling of conserved residues in transmembrane region 5. *Mol. Pharmacol.* **2000**, *58*, 877−886.
(39) Shen, Y.; Monsma, F. J., Jr.; Metcalf, M. A.; Jose, P. A.; Hamblin, M. W.; Sibley, D. R. Molecular cloning and expression of a 5-hydroxytryptamine7 serotonin receptor subtype. *J. Biol Chem.* **1993**, *268*, 18200−18204.
(40) Snyder, J.P.; Rao, S.N.; Koehler, K.F.; Vedani, A.; Pelliciari, R. APOLLO Pharmacophores and the pseudoreceptor concept. In *Trends in QSAR and Molecular Modeling 92*; Wermuth, C. G., Ed.; ESCOM: Leiden, 1993; pp 44−51.
(41) Speeter, M. E.; Anthony, W. C. The action of oxalyl chloride on indoles: a new approach to tryptamines. *J. Am. Chem Soc.* **1954**, *76*, 6208−6210.
(42) Steiner, T.; Koellner, G. Hydrogen Bonds with p-Acceptors in Proteins: Frequencies and Role in Stabilizing Local 3-D Structures. *J. Biol. Chem.* **2001**, *305*, 535−557.
(43) Still, W. K.; Tempczyk, A.; Hawley, R. C.; Hendrickson, T. Semianalytical treatment of solvation for molecular mechanics and dynamics. *J. Am. Chem. Soc.* **1990**, *112*, 6127−6129.
(44) Thomas David, R.; Gittins Susan, A.; Collin Lissa, L.; Middlemiss Derek, N.; Riley Graham; Hagan Jim; Gloger Israel; Ellis Catherine, E.; Forbes Ian, T.; Brown Anthony, M. Functional characterisation of the human cloned 5-HT7 receptor (long form): Antagonist profile of SB-258719. *Br. J. Pharmacol.* **1998**, *124*, 1300−1306.
(45) Thomas, D. R.; Atkinson, P. J.; Hastie, P. G.; Roberts, J. C.; Middlemiss, D. N.; Price, G. W. [3H]-SB-269970 radiolabels 5-HT7 receptors in rodent, pig and primate brain tissues. *Neuropharmacology* **2002**, *42*, 74−81.
(46) Thomas, D. R.; Atkinson, P. J.; Ho, M.; Bromidge, S. M.; Lovell, P. J.; Villani, A. J.; Hagan, J. J.; Middlemiss, D. N.; Price, G. W. [H-3]-SB-269970 − A selective antagonist radioligand for 5-HT7 receptors. *Br. J. Pharmacol.* **2000**, *130*, 409−417.
(47) Vermeulen, E. S.; Schmidt, A. W.; Sprouse, J. S.; Wikstrom, H. V.; Grol, C. J. Characterization of the 5-HT(7) receptor. Determination of the pharmacophore for 5-HT(7) receptor agonism and CoMFA-based modeling of the agonist binding site. *J. Med. Chem.* **2003**, *46*, 5365−5374.
(48) Wesolowska, A. In the search for selective ligands of 5-HT5, 5-HT6 and 5-HT7 serotonin receptors. *Pol. J. Pharmacol.* **2002**, *54*, 327−341.

JM049743B